VERIFICATION OF A COMMERCIAL MONTE CARLO BASED ORGAN AND EFFECTIVE DOSES CALCULATION IN MULTI-DETECTOR COMPUTED TOMOGRAPHY USING THERMOLUMINESCENT DOSIMETER

WORANUT IAMPA

A THESIS SUBMITTED IN PARTIAL FULFILLMENT
OF THE REQUIREMENTS FOR
THE DEGREE OF MASTER OF SCIENCE
(RADIOLOGICAL TECHNOLOGY)
FACULTY OF GRADUATE STUDIES
MAHIDOL UNIVERSITY
2008

Thesis
Entitled

VERIFICATION OF A COMMERCIAL MONTE CARLO BASED ORGAN AND EFFECTIVE DOSES CALCULATION IN MULTI-DETECTOR COMPUTED TOMOGRAPHY USING THERMOLUMINESCENT DOSIMETER

.....

Miss Woranut Iampa
Candidate

.....

Asst.Prof. Napapong Pongnapang,
Ph.D. (Medical Physics)
Major-Advisor

.....

Assoc.Prof. Chavalit Wongse-ek,
M.Sc. (Physics)
Co-Advisor

.....

Prof. Banchong Mahaisavariya,
M.D.
Dean
Faculty of Graduate Studies

.....

Asst.Prof. Napapong Pongnapang,
Ph.D. (Medical Physics)
Chair
Master of Science Programme in
Radiological Technology
Faculty of Medical Technology

Thesis
Entitled

VERIFICATION OF A COMMERCIAL MONTE CARLO BASED ORGAN AND EFFECTIVE DOSES CALCULATION IN MULTI-DETECTOR COMPUTED TOMOGRAPHY USING THERMOLUMINESCENT DOSIMETER

was submitted to the Faculty of Graduate Studies, Mahidol University
for the Degree of Master of Science (Radiological Technology)
on
March 28, 2008

W. Iampa
.....
Miss Woranut Iampa
Candidate

Sivalee Suriyapee
.....
Assoc.Prof. Sivalee Suriyapee,
M.Eng. (Nuclear Technology)
Chair

.....
Asst.Prof. Napapong Pongnapang,
Ph.D. (Medical Physics)
Member

C. Wongse-ek
.....
Assoc.Prof. Chavalit Wongse-ek,
M.Sc. (Physics)
Member

B. Mahaisavariya
.....
Prof. Banchong Mahaisavariya,
M.D.
Dean
Faculty of Graduate Studies
Mahidol University

Virapong
.....
Assoc.Prof. Virapong Prachayasittikul,
Ph.D. (Microbiology)
Dean
Faculty of Medical Technology
Mahidol University

ACKNOWLEDGEMENT

The success of this thesis can be attributed to the extensive support and assistance from my major advisor, Asst.Prof. Napapong Pongnapang, and my co-advisor, Assoc.Prof. Chavalit Wongse-ek. I would like to express my sincere gratitude and deep appreciation to them for their supervision, guidance, and encouragement throughout this thesis.

I would like to thank Assoc.Prof. Sivalee Suriyapee, Chairperson of the thesis examination committee, from Department of Radiology, Faculty of Medicine, Chulalongkorn University for kindness to be the chairperson of this thesis examination committee and suggestion for improvement of this thesis.

I would like to thank Mr. Thanapat Nopsopon, Electronics Associate of Faculty of Medical Technology, Mahidol University, for their assistances and kind support to make some materials necessary to this thesis.

I would like to thank the staffs from Biomedical Instrumentation Center, Mahidol University for their assistances and kind support to make some materials necessary to this thesis.

I would like to thank my friends for their assistance and encouragement throughout this thesis. Finally, I am grateful to my family for their financial support, entirely care, and love. The usefulness of this thesis, I dedicate to my parents, my brother, and all the teachers who have taught me since my childhood.

Woranut Iampa

VERIFICATION OF A COMMERCIAL MONTE CARLO BASED ORGAN AND EFFECTIVE DOSES CALCULATION IN MULTI-DETECTOR COMPUTED TOMOGRAPHY USING THERMOLUMINESCENT DOSIMETER

WORANUT IAMPA 4837707 MTRT/M

M.Sc. (RADIOLOGICAL TECHNOLOGY)

THESIS ADVISORS: NAPAPONG PONGNAPANG, Ph.D. (MEDICAL PHYSICS), CHAVALIT WONGSE-EK, M.Sc. (PHYSICS)

ABSTRACT

This study was carried out to verify the accuracy and the limitations of a WinDose® program version 2.1a based on the Monte Carlo calculation using thermoluminescent dosimeters (TLDs). The study was performed on a GE LightSpeed Plus Multi-Detector Computed Tomography (MDCT) scanner in the examinations of head, chest, upper and lower abdomen. Calibrated TLDs-100H rods were used to measure absorbed doses in Alderson Rando phantom. Effective doses were calculated according to the International Commission on Radiological Protection (ICRP) Publication 60. For the WinDose® calculation, CT air kerma index free-in-air was measured and used as a parameter of normalization quantity.

Results showed that organ doses in scan sections calculated from the WinDose® were in agreement within ±16% as compared to those determined by the TLD, except for the doses of breast in the chest examination and some extended organs in the examinations of upper and lower abdomen. The doses outside scan sections were lower than those from the TLD. The effective doses from the WinDose® were 21-33% lower than those from the TLD in all examinations except for the head examination.

WinDose® program version 2.1a can be used to calculate the organ and effective doses in CT examinations of chest, upper and lower abdomen. The head examination or examination with various scan sections should be separately calculated.

KEY WORDS: THERMOLUMINESCENT DOSIMETER / ORGAN DOSE / EFFECTIVE DOSE / MONTE CARLO CALCULATION / COMPUTED TOMOGRAPHY

75 pp.

การพิสูจน์ความถูกต้องของโปรแกรม MONTE CARLO ในการคำนวณปริมาณรังสีที่อวัยวะได้รับและปริมาณรังสียังผล จากการตรวจด้วยเครื่องเอกซเรย์คอมพิวเตอร์ชนิดหลายหัววัด โดยใช้การวัดรังสีแบบเทอร์โมลูมิเนสเซนส์ (VERIFICATION OF A COMMERCIAL MONTE CARLO BASED ORGAN AND EFFECTIVE DOSES CALCULATION IN MULTI-DETECTOR COMPUTED TOMOGRAPHY USING THERLUMINESCENT DOSIMETER)

วรนุช เอี่ยมปา 4837707 MTRT/M

วท.ม. (รังสีเทคนิค)

คณะกรรมการควบคุมวิทยานิพนธ์: นภาพงษ์ พงษ์นภางค์, Ph.D. (MEDICAL PHYSICS), ชวลิต วงษ์เอก, M.Sc. (PHYSICS)

บทคัดย่อ

งานวิจัยนี้เป็นการพิสูจน์ความถูกต้องและหาข้อจำกัดของโปรแกรม WinDose® version 2.1a ในการคำนวณปริมาณรังสีที่อวัยวะได้รับและปริมาณรังสียังผล จากเครื่องเอกซเรย์คอมพิวเตอร์ชนิดหลายหัววัด โดยการวัดรังสีแบบเทอร์โมลูมิเนสเซนส์ (TLD) ในหุ่นจำลองมนุษย์ในการตรวจทั่วไป 4 ส่วน คือ ศรีษะ ช่องอก ช่องท้องส่วนบน และช่องท้องส่วนล่าง

จากการศึกษาพบว่า ปริมาณรังสีดูดกลืนในอวัยวะที่ได้รับรังสีโดยตรง ที่ได้จากการคำนวณของโปรแกรม WinDose® มีความสอดคล้องกับปริมาณรังสีดูดกลืนในอวัยวะที่ได้จาก TLD อยู่ในช่วง ±16% ยกเว้นปริมาณรังสีในเต้านมในการตรวจช่องอก และในบางอวัยวะที่อยู่ทั้งในช่องท้องส่วนบนและส่วนล่าง และพบว่าปริมาณรังสีของอวัยวะที่ได้รับเฉพาะรังสีกระเจิง ที่ได้จากการคำนวณของโปรแกรม WinDose® มีค่าน้อยกว่าที่ได้จาก TLD นอกจากนี้ปริมาณรังสียังผลที่ได้จาก WinDose® มีค่าน้อยกว่าที่ได้จาก TLD เท่ากับ 21-33% ในทุกการตรวจ ยกเว้นการตรวจเอกซเรย์คอมพิวเตอร์ส่วนศรีษะ

จากการศึกษาครั้งนี้ สามารถใช้โปรแกรม WinDose® เพื่อคำนวณปริมาณรังสีที่อวัยวะได้รับและปริมาณรังสียังผลจากเครื่องเอกซเรย์คอมพิวเตอร์ชนิดหลายหัววัดในการตรวจช่องอก ช่องท้องส่วนบน และช่องท้องส่วนล่างได้ การคำนวณปริมาณรังสีในการตรวจส่วนศรีษะหรือการตรวจอื่นซึ่งประกอบด้วยช่วงของการตัดภาพหลายช่วง โดยใช้เทคนิคการตรวจที่ต่างกันในการตรวจครั้งเดียว ควรแยกการคำนวณปริมาณรังสีออกจากกันในแต่ละช่วงของการตัดภาพ

75 หน้า

CONTENTS

LIST OF TABLES

LIST OF TABLES (Continued)

LIST OF TABLES (Continued)

LIST OF FIGURES

LIST OF FIGURES (Continued)

LIST OF ABBREVIATIONS

Abbreviations	Term
CT	Computed tomography
MDCT	Multi-detector-row computed tomography
CTDI	Computed tomography dose index
PMMA	Polymethyl methacrylate
TLD	Thermoluminescent dosimeter
Temp.	Temperature
kVp	Peak tube voltage
mmAl	millimeters Aluminum
nC	nanoCoulomb
mAs	Tube-current time product
mGy	miliGray
mSv	miliSievert
HU	Houndsfield Units
SD	Standard deviation

CHAPTER I
INTRODUCTION

Recent development in computed tomography (CT) increases the improvement in clinical diagnosis and also lead to high radiation doses to patients. The CT examinations contribute the largest radiation dose to diagnostic x-ray examinations (1-6), especially in multi-detector-row CT or MDCT (7, 8). The radiation doses to the patients can be assessed in terms of organ doses and effective doses which indicate risks of biological injury (9-11).

Generally, there are three common CT dosimetry approaches used to determine the radiation doses. These approaches are determination of Computed Tomography Dose Index (CTDI) (12, 13), thermoluminescent dosimeter (TLD) measurement, and Monte Carlo calculation. The CTDI measurement using an ionization chamber with standard PMMA (polymethyl methacrylate) phantom is normally used for quality assurance (14) and does not provide a direct assessment of the risks to the patients resulting from CT examinations.

The second dosimetric method is TLD measurement in an anthropomorphic phantom such as Alderson Rando phantom. Because of their small size and capacity of storing dose information over longer periods of time, the TLDs are suitable for the dose measurement on the patients. In diagnostic radiology, the TLDs-100H of LiF: Mg, Cu, P are commonly used due to their characteristics of low x-ray energy response (15, 16), high sensitivity, low detection threshold, and high signal-to-noise ratio (17). There were many studies (18-22) measuring absorbed doses to organs and effective doses in the CT examinations by using the TLD measurement in anthropomorphic phantom

Another approach is a Monte Carlo calculation of radiation transport in a mathematical phantom. The Monte Carlo technique is a computational method used to simulate and record the energy deposition of x-ray photons from the photon interactions of photoelectric effect and Compton scattering in the computational

models of human body (9). All energy depositions from primary and scattered photon are divided by organ mass to obtain the organ doses. The organ doses are normalized to organ dose conversion coefficients, corresponding to the normalization quantity (23).

Sources of the organ dose conversion coefficients for CT examinations are reports produced by the German National Research Center for Environment and Health (GSF) and reports produced by the National Radiological Protection Board (NRPB). The organ dose conversion coefficients in the GSF Reports are obtained from the Monte Carlo calculation with male and female phantoms namely ADAM and EVA phantoms, respectively, modified from an original medical internal radiation dose (MIRD) phantom (24) in three radiation qualities of the CT scanners (25). The organ dose conversion coefficients in the NRPB Reports are obtained from the Monte Carlo calculation with Cristy hermaphrodite phantom for twenty-three sets of exposure conditions suitable for twenty-seven CT scanner models (26, 27).

From these CT dosimetry approaches, the TLD measurement in anthropomorphic phantom is mostly appropriate to determine the patient doses in CT. The TLD measurement can represent radiation attenuation, radiation scattering and dose distribution corresponding to various organs or tissues of the human body in clinical practice. However, the TLD measurement is a laborious and time consuming technique.

Therefore, there are many studies (19, 20, 22, 28, 29) which apply the organ dose conversion coefficients from the Monte Carlo calculation with the normalization quantity to calculate the organ doses and the effective doses. Moreover, the organ dose conversion coefficients based on Monte Carlo simulation are developed in form of a program or code to calculate the organ and effective doses, for example, CTDOSE (31), ImPACT (32), CT-EXPO (33), WinDose (34). The ImPACT and CT-EXPO were used to calculate the effective doses by Van der Molen et al., 2007 (30) and Brix et al., 2004 (22).

The WinDose® version 2.1a (34) is a personal computer program for calculating the organ doses and the effective doses from the CT examinations (35). The organ dose conversion coefficients in the WinDose® calculation are derived from the GSF Report resulting from the Monte Carlo simulation of the three radiation qualities. The

coefficients of each organ are tabulated for a single axial 1 cm slice thickness per a unit of CT air kerma index. The organ doses are calculated from a summation of organ dose conversion coefficients in any scan sections multiplied by the CT air kerma index free-in-air specific to the CT scanner.

Since the organ dose conversion coefficients published by the GSF Report were derived from the specific CT scanners in 1989 which may be differ from the current CT scanners in terms of scanner geometry, a total filtration, a beam shaping device including the radiation quality. Therefore, this study was carried out to verify an accuracy and limitations of a commercial Monte Carlo based organ and effective doses calculation namely WinDose® program version 2.1a by using the TLD measurement in Alderson Rando phantom.

CHAPTER II
OBJECTIVES

This study consists of the following objectives.

1. To determine the organ doses and the effective doses in the examinations of head, chest, upper abdomen, and lower abdomen from a multi-detector computed tomography (MDCT) scanner by using the TLD measurement in Alderson Rando phantom and the dose calculation of WinDose® program version 2.1a.

2. To verify the accuracy of the organ doses and the effective doses calculated from the WinDose® program by comparison with the doses resulting from the TLD measurement in the examinations of head, chest, upper abdomen, and lower abdomen.

3. To study the limitations of the organ doses and the effective doses calculation of the WinDose® program version 2.1a.

CHAPTER III
LITERATURE REVIEW

The dosimetry approaches commonly used for patient dose measurement in CT are the TLD measurement in Alderson Rando phantom and the organ and effective doses calculation based on Monte Carlo simulation. The TLD measurement is a suitable method for the patient dose measurement but it is laborious and time consuming technique. Therefore, there were many studies which used the organ dose conversion coefficients combined with the normalization quantity to calculate the organ doses and the effective doses.

In 1999, Hidajat et al. (28) determined the organ doses and the effective doses by using the CTDI free-in-air combined with the organ dose conversion coefficients published by the GSF Report. The CTDI free-in-air were measured for a nominal slice thickness of 10 mm and scan parameters of 100 mAs at 120 kVp and 137 kVp. The doses were calculated in the various examinations which were the examinations of skull, neck, thorax, upper abdomen, pelvis, and whole abdomen on a Somatom Plus CT scanner. The effective dose in each examination was calculated according to the Recommendation of the International Commission on Radiation Protection (ICRP) Publication 60 (36). The organ doses were calculated for the organs located in the scan sections in each examination and the effective doses were 1.00, 1.95, 5.37, 3.71, 5.48, and 9.20 mSv for the examinations of skull, neck, thorax, upper abdomen, pelvis, and whole abdomen, respectively.

In 2001, Peter F. (37) determined the organ doses and the effective doses in the examinations of head and abdomen on a Siemens Somatom Plus 4 CT scanner. The doses were calculated by using CTDI measurement in phantom with EGS4-VLSI (Electron Gamma Shower Release 4 for Very Large Scale Images) code based on a voxel phantom. The CTDI values were measured in PMMA (polymethyl methacrylate) head and body phantoms for the examinations of head and abdomen, respectively. The CTDI measurement for the head examination was scanned with a 10 mm slice

thickness at 120 kVp and 390 mAs. The CTDI measurement for the abdomen examination was scanned with a 10 mm slice thickness at 120 kVp and 200 mAs. The effective doses were calculated according to the Recommendation of the ICRP Publication 60. As a consequence, the effective dose in the head examination was 0.75 ± 0.01 mSv and the largest contributors to the effective dose were red bone marrow, bone surface, and thyroid. The effective dose in the abdomen examination was 3.85 ± 0.28 mSv and the largest contributors to the effective dose were colon, stomach, and liver.

In 2007, Van der Molen et al. (30) calculated the effective doses by using the normalized CTDI free-in-air and the ImPACT dose calculator in the examinations of brain, chest, and abdomen. The CTDI free-in-air values were measured at 80, 100, 120, and 140 kVp with all available slice collimation settings in spiral scan mode from the four CT scanners with 16-slice. As a result, the effective doses in the examinations of brain, chest, and abdomen on a GE LightSpeed 16 CT scanner were 2.3, 4.1, and 7.8 mSv, respectively. The mean effective doses from the four CT scanners were 1.9, 3.8, and 7.2 mSv for the examinations of head, chest, and abdomen, respectively.

Moreover, the organ and effective doses calculation based on the Monte Carlo simulation was studied and compared with the dose measurement by using the TLD. In 1994, Geleijns et al. (18) studied comparison of the two CT dosimetric methods which were the CTDI values combined with the organ dose conversion coefficients and the doses measurement by using the TLD in Alderson Rando phantom. The organ doses and the effective doses were determined in the examinations of head, thorax, and abdomen on a Phillips Tomoscan LX CT scanner.

For the TLD measurement, the TLD-100 chips of Harshaw were calibrated with a Cs-137 source and corrected for energy dependence. The TLDs about 200 chips were used to measure the absorbed doses in various organs according to an atlas on CT anatomy in a small female Rando phantom with a length of 163 cm and a weight of 54 kg. The effective doses were calculated according to the ICRP Publication 60.

For the organ doses calculation by using the CTDI combined with the organ dose conversion coefficients, the CTDI free-in-air values were measured with a Capintec PC-4P ionization chamber at a central axis of rotation. The organ doses were calculated from the CTDI free-in-air combined with the organ dose conversion

coefficients published by the GSF and the NRPB Reports. Some organ doses of thyroid, lung, breast, stomach, liver, bladder, and red bone marrow calculated from the CTDI and organ dose conversion coefficients were compared with those resulting from the TLD in the examinations of thorax and abdomen. The results showed that the effective doses calculated from the CTDI and organ dose conversion coefficients for a mathematical phantom were up to 40% lower than those determined by the TLD measurement in Rando phantom.

In 2004, the organ and the effective doses calculation based on the Monte Carlo simulation was compared with the dose measurement by using the TLD in the study of Groves et al. (21). Standard 3 mm by 3mm by 0.8 mm lithium fluoride TLD chips calibrated with a diagnostic energy at the central axis of rotation of the CT scanner were used to measure the absorbed doses in Rando phantom. The Rando phantom and the 65 TLDs were performed with a whole body examination which was scanned from vertex to mid thigh with a 1.5 mm slice thickness in helical mode on a Siemens Somatom Sensation 16 CT scanner. The effective doses were calculated according the Recommendation of ICRP 60.

The organ dose calculation based on Monte Carlo simulation was calculated by the ImPACT calculator version 0.99q which the CTDI values were combined with the organ dose conversion coefficients produced by the NRPB Report. The organ doses resulting from both methods were compared according to the organs recommended by the ICRP 60. The effective doses determined by the TLD were 23.6 and 20.8 mSv for men and women, respectively. In conclusion, the mean effective dose of 22.2 mSv resulting from the TLD measurement in Rando phantom was 18% higher than the effective dose of 18.8 mSv from the ImPACT calculation.

In 2004, Brix et al. (22) determined the effective doses by using the a personal computer program namely CT-EXPO and by using the TLD measurement in the examinations of head, chest, and pelvis on a variety of single-slice spiral CT (SSCT) and multi-slice spiral CT (MSCT). The dose calculation and dose measurement were performed on ten different CT scanners which were comprised of four 1-slice, four 4-slice, and two 16-slice CT scanners.

The TLD-100 rods and chips were calibrated for the absorbed dose in water using conventional x-ray system with 120 kVp and a total filtration of 5 mmAl. The 100

TLD rods were used to measure the absorbed doses inside the Alderson Rando phantom and more than 83 TLD chips were used to measure the doses at the surface of phantom. Then, the effective doses were calculated according to the ICRP Publication 60.

The effective doses resulting from the CT-EXPO program were calculated by the weighted CTDI values combined with the scanning parameters and scanner-specific conversion factors. The scanner-specific conversion factors were derived from the organ dose conversion coefficients calculated for the mathematical model of ADAM and EVA phantoms. The results showed that the effective doses calculated by using the CT-EXPO program deviated less than 32% from those determined by the TLD measurement.

Most of these studies compared the dose calculation based on Monte Carlo simulation with the TLD measurement in terms of the effective dose in each examination. Therefore, this study was carried out to verify the accuracy in both organ and effective doses calculated from the WinDose® program by using the TLD measurement.

CHAPTER IV
MATERIALS AND METHODS

4.1 Materials

4.1.1 Multi-detector computed tomography (MDCT) scanner

Multi-detector computed tomography (MDCT) scanner, 4-detector rows, Model LightSpeed Plus manufactured by General Electric (GE) shown in Figure 4.1.1 was used in this study. Quality equivalent filtration of the CT system with performix x-ray tube is 4.75 mmAl measured at 70 kVp. The kV choices of this CT system consist of 80, 100, 120, 140 kV. The MDCT scanner was performed quality control according to American Association of Physicists in Medicine (AAPM) Report No. 39 (38).

4.1.2 Thermoluminescent dosimeters (TLDs)

Thermoluminescent dosimeters-100H of LiF: Mg, Cu, P or TLDs-100H, rod type, shown in Figure 4.1.2 manufactured by Thermo Electron Corporation Radiation Measurement and Protection were used to measure the absorbed dose in Alderson Rando phantom. A dimension of TLD is 1 mm diameter and 6 mm long.

4.1.3 Thermoluminescent dosimeters system

A) Automatic TLD reader

The Harshaw automatic TLD reader Model 5500 shown in Figure 4.1.3.A is capable of reading 50 dosimeters per loading of dosimeter carrier or disk. The TLD reader was operated with the Windows Radiation Evaluation and Management System (WinREMS^{TM}) software on a personal computer. Reference light stability of the reader in short term is less than 0.5% variation based on 1 standard deviation of 10 consecutive readings performed at a constant temperature. For long term with 0.5 to 110 hours, the reference light stability is 2% of maximum deviation. Dark current is less than 50 µGy, ^{137}Cs equivalent. The TLD reader Model 5500 must be operated

with prepurified (99.995%) and dry nitrogen supply. The nitrogen pressure and flow rate are 2.8 to 6.3 kg/cm^2 or 40 to 90 psi and 400 L/H, respectively.

Figure 4.1.1 Multi-detector computed tomography scanner Model GE LightSpeed Plus

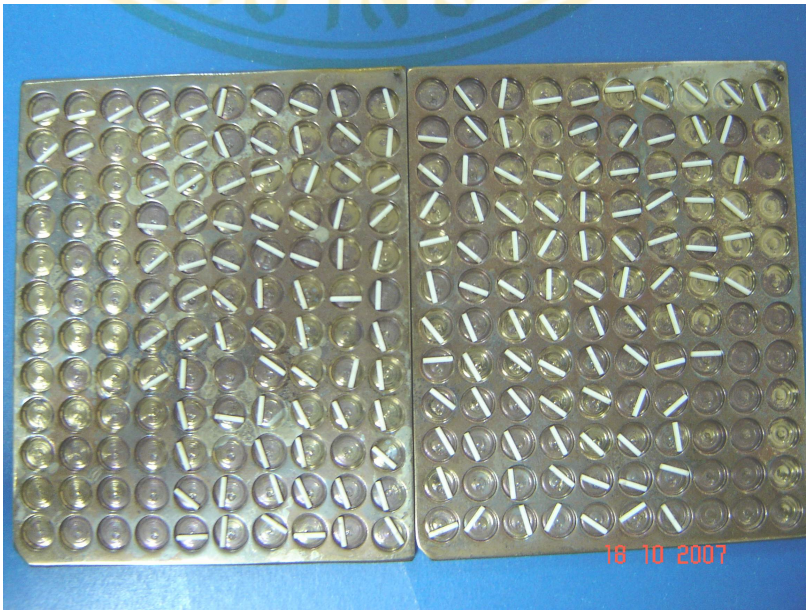

Figure 4.1.2 Thermoluminescent dosimeters (TLDs)-100H (rod type)

Figure 4.1.3.A Automatic reader Model 5500 with WinREMS™

B) TLD annealing oven

TLD annealing oven of PTW-FREIBURG shown in Figure 4.1.3.B was used to anneal the TLDs to eliminate residual TL signal. Temperature accuracy of the annealing oven is 0.5% ± 1 digit. The TLD annealing oven was controlled by THELDO program used to create and process heating program.

4.1.4 Alderson Rando phantom

A male Alderson Rando phantom shown in Figure 4.1.4 with 2.5 mm thickness was used with the TLDs to measure the absorbed doses. The phantom of 175 cm tall and 73.5 kg weight consists of 36 slices with the number 0 to 35 and are modeled according to International Commission on Radiation Units and Measurements (ICRU) Report 44 with tissue-equivalent material.

4.1.5 Ionization chamber and electrometer

An ionization chamber type TM 30009 with a volume of 3.14 cm^3 as shown in Figure 4.1.5.A manufactured by PTW-FREUBURG was used to measure the absorbed doses for TLD calibration and measurement of CT air kerma index. Energy dependence of ionization chamber is 1 at 70 keV. Uncertainty of calibration factor is ± 5%. The ionization chamber was used together with a PTW-NOMEX (Noninvasive

Measurements of X-Ray Beams) electrometer shown in Figure 4.1.5.B. The digital resolution of the electrometer is 1%.

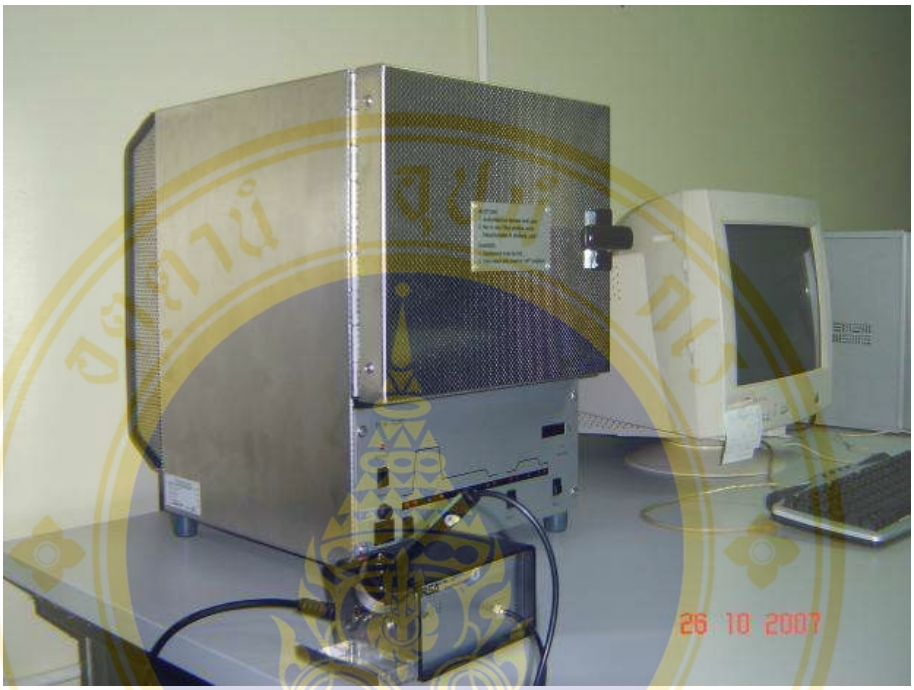

Figure 4.1.3.B TLD annealing oven of PTW-FREIBURG

Figure 4.1.4 Male Alderson Rando phantom

Figure 4.1.5.A Ionization chamber type TM 30009 with a volume of 3.14 cm^3

Figure 4.1.5.B Electrometer PTW-NOMEX

4.1.6 X-ray system

An x-ray system of Quantum Medical Imaging with x-ray generator Model QG 32 shown in Figure 4.1.6 was used to expose the TLDs to determine their correction factors for sensitivity. A total filtration of the x-ray tube is 2.9 mmAl at 80 kVp. The x-ray system was performed the quality control according to the National Council on

Radiation Protection and Measurement (NCRP) Report No. 99 (39).

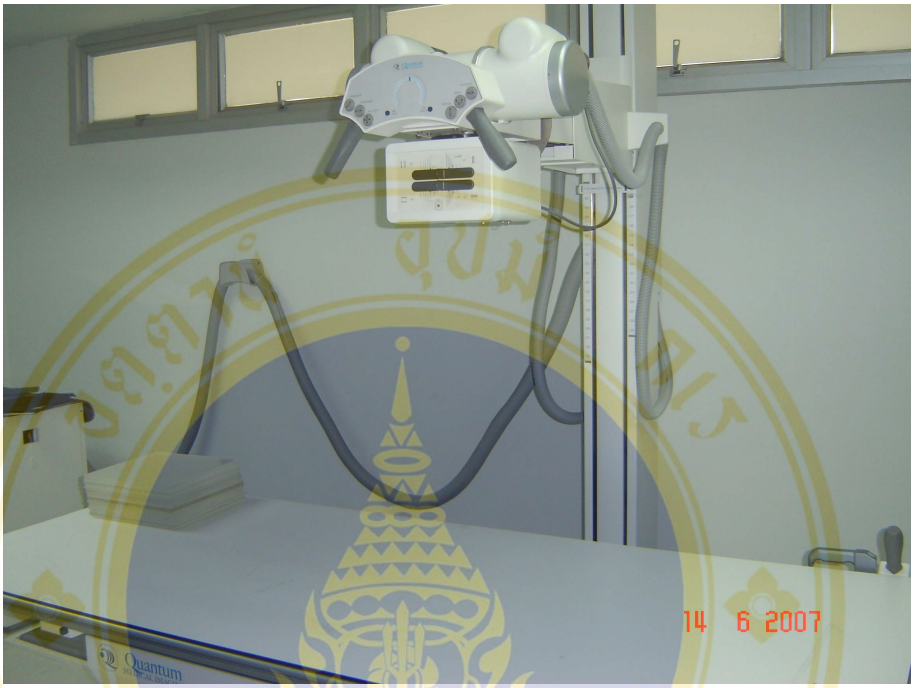

Figure 4.1.6 X-ray system of Quantum Medical Imaging

4.1.7 WinDose® program version 2.1a

The WinDose® program version 2.1a (34) shown in Figure 4.1.7 was used to calculate the organ doses and the effective doses in computed tomography. The organ dose conversion coefficients are based on the Monte Carlo (MC) simulations for anthropomorphic mathematical phantoms which are obtained from the GSF Report. The mathematical phantoms are based on the original Medical International Radiation Dose (MIRD) phantom and modified as Adam and Eva phantoms including sex-specific characteristics.

4.1.8 CT head phantom

A CT head PMMA (polymethyl methacrylate) phantom shown in Figure 4.1.8 manufactured by PTW-FREIBURG was used in the TLD calibration. The CT head phantom has a 6 cm diameter and 15 cm long.

4.1.9 CatPhan® 600 phantom

CTP 404 Module of CatPhan® 600 phantom (40) shown in Figure 4.1.9.A

manufactured by the Phantom Laboratory, Inc. was used to determine effective energy required as an input parameter for the WinDose® program. The CTP 404 Module consists of seven high contrast sensitometric targets surrounding the wire slice thickness ramps. The high contrast sensitometric targets as shown in Figure 4.1.9.B were made from Teflon, acrylic, low density polyethylene (LDPE), and air.

Figure 4.1.7 WinDose® program version 2.1a

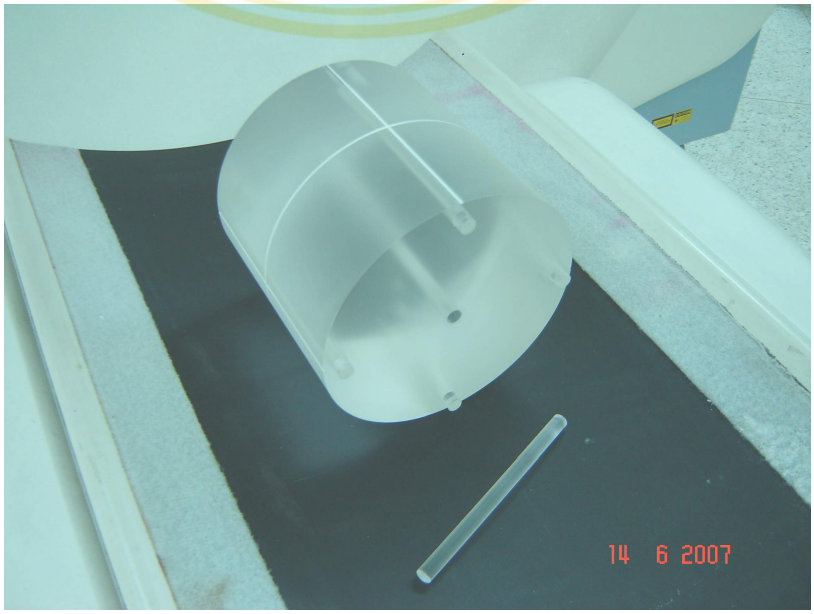

Figure 4.1.8 CT head phantom

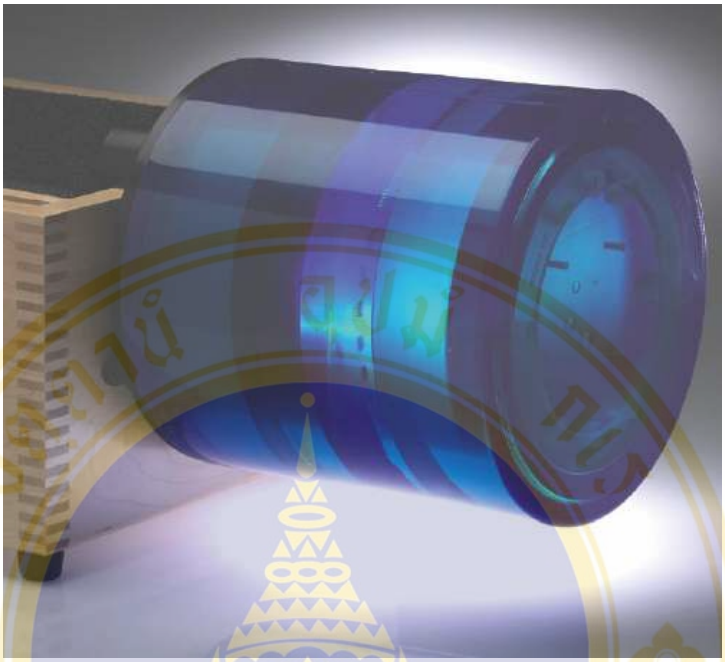

Figure 4.1.9.A CatPhan® 600 phantom (40)

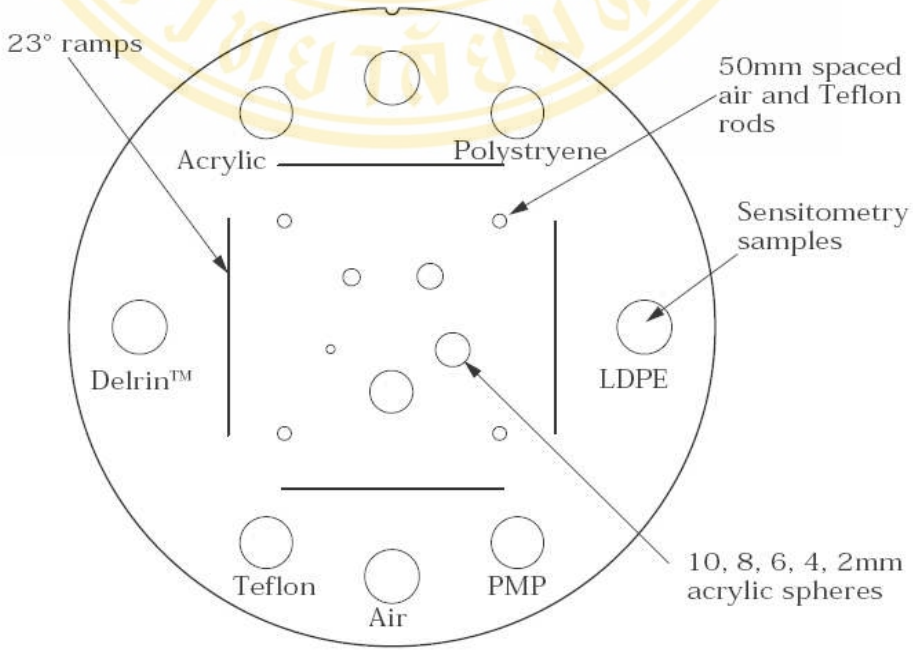

Figure 4.1.9.B Cross-sectional image of CTP 404 Module (40)

4.2 Methods

4.2.1 TLD preparation

TLD preparation for the TLD measurement was described as the following procedures.

A) Determination of minimum detectable dose

The 180 rods of TLDs-100H were annealed at 240 °C for 10 minutes. The TLDs were annealed for 4 times to eliminate the residual signals and were read background TL signal according to Time Temperature Profile of Harshaw as shown in Table 4.2.1.A. The TLDs were annealed and read for six times.

Minimum detectable dose was calculated by summation of the average background TL signal of all TLDs and the three times of standard deviation (3SD) of all background TL signal. The average background TL signal is 0.212 nC and the 3SD of TL signal is 0.143 nC. Therefore, according to the calibration curve, the minimum detectable dose is 0.355 nC or 0.085 mGy.

Table 4.2.1.A Time Temperature Profiles of Harshaw for TLDs-100H

Preheat		**Acquisition**			**Annealing**	
Temp. (°C)	**Time (s)**	**Rate (°C/s)**	**Maximum Temp. (°C)**	**Time (s)**	**Temp. (°C)**	**Time (s)**
145	10	10	260	23 1/3	260	10

B) Grouping and determination of correction factors for sensitivity

All TLDs were put in two acrylic plates with 8 x 10 cm and were exposed from the x-ray system with 120 kVp, 40 mAs at 50 cm source-to-skin distance (about 1 R) and field size of 25 x 30 cm. All TL signals were read and recorded. This process was repeated for three times. The averaged TL signal of each TLD was recorded in ascending number and every twelve TL signals were grouped with 3% of SD in each group. The correction factor for sensitivity of each TLD group was calculated by following equation.

$$\text{Correction factor for sensitivity} = X / X_i \qquad \text{Equation 4.2.1}$$

Where X is average TL signal of all TLDs

X_i is average TL signal of TLDs in the i^{th} group

Therefore, all TLDs were classified into 21 groups and the average TL signal of all TLDs was 249.11 nC. The correction factors for sensitivity of each group range in 0.58-1.88 as shown in Appendix A.

C) TLD calibration

TLDs were calibrated with diagnostic energy from MDCT scanner. The TLD calibration was described as the following procedures.

1) The CT head phantom was set according to AAPM No. 39 (38). The ionization chamber was used to measure the absorbed doses in a central hole of CT head phantom shown in Figure 4.2.1.A with a single rotation and a single slice of 10 mm thickness at 120 kVp and with various mAs values to receive the different absorbed doses. The absorbed doses were calculated according to Equation 4.2.2. The mAs values and the corresponding absorbed doses in mGy are shown in Table 4.2.1.B.

$$\text{Absorbed dose (mGy)} = \text{Reading} \cdot N_a \cdot k_Q \cdot k_{T,P} \cdot f \qquad \text{Equation 4.2.2}$$

Where N_a is an exposure calibration factor (1.00 at 140 kV with total filtration of 12.5 mmAl)

k_Q is a correction factor for radiation quality

$k_{T,P}$ is a correction factor for temperature and pressure

f is a conversion factor used to convert exposure to absorbed dose (0.00876 mGy/mR)

2) The 5 TLDs and 24 TLDs were vertically loaded in a central region of TLD holder with space of 2 mm and in a peripheral region of TLD holder with space of 4 mm, respectively. The TLD holder were inserted in the head phantom as shown in Figure 4.2.1.B and were calibrated with the same condition as the measurement of absorbed doses in the CT head phantom according to the nine values of absorbed dose described in Table 4.2.1.B.

3) The TL signals of calibrated TLDs were read, averaged, and multiplied by the correction factor for sensitivity of each TLD shown in Appendix A.

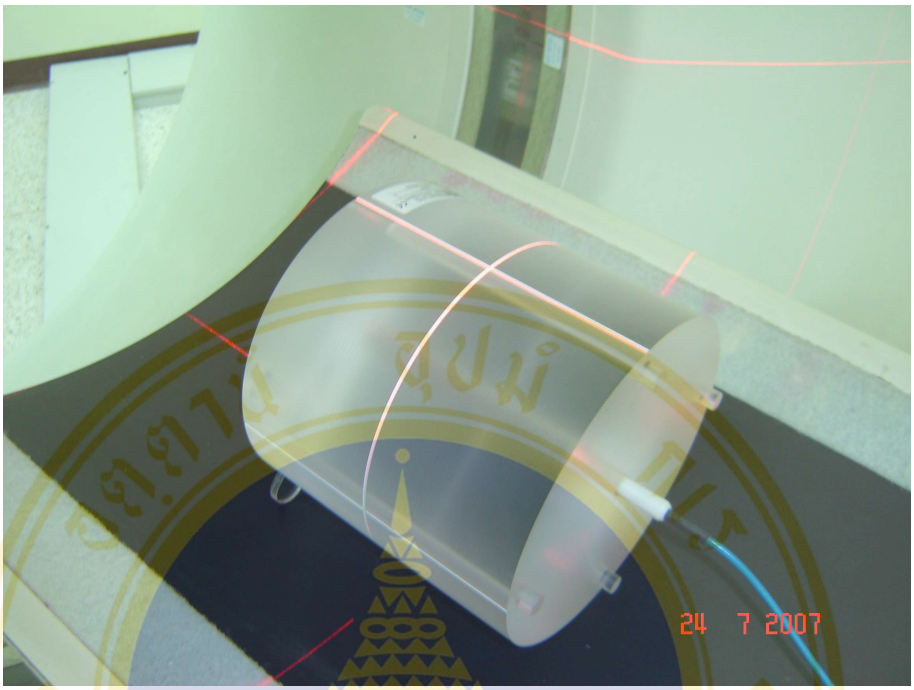

Figure 4.2.1.A Absorbed dose measurement in a central hole of CT head phantom

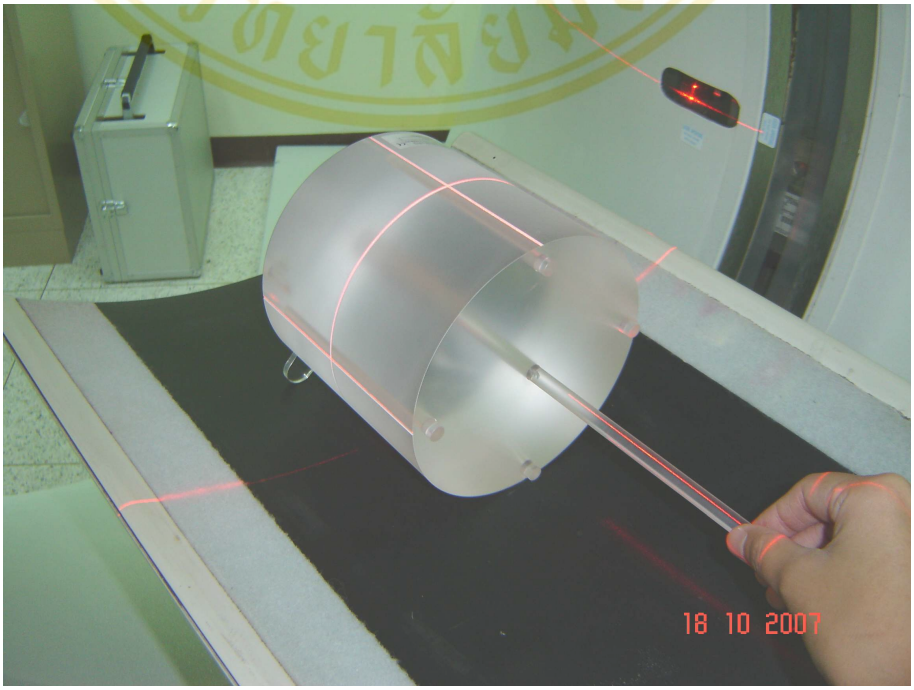

Figure 4.2.1.B TLD holder inserted in CT head phantom

Table 4.2.1.B Values of mAs and the corresponding absorbed doses in mGy at 120 kV

Tube voltage (kV)	Tube current (mA)	Exposure time (s)	mAs	Absorbed doses (mGy)
120	10	0.5	5	0.332
120	10	0.8	8	0.532
120	20	0.8	16	1.088
120	30	1	30	2.051
120	30	2	60	4.100
120	50	2	100	7.094
120	70	2	140	9.905
120	90	2	180	12.688
120	160	2	320	22.446
120	240	2	480	35.414
120	320	2	640	47.288
120	400	2	800	58.934

4) The corrected TL signals were plotted against the position of each TLD as a profile of TL signal correlated with the absorbed dose. An example of the profile correlated with 12.688 mGy is shown in Figure 4.2.1.C. The total TL signal of each value of absorbed dose was determined by a summation of area under the profile.

5) The total TL signal in a unit of nC•mm was divided by the slice thickness of 10 mm to determine the TL signal corresponding to the absorbed dose in the Table 4.2.1.B. The absorbed doses in mGy and the corresponding TL signals are shown in Appendix B.

6) The absorbed doses in mGy were plotted against the corresponding TL signals in nC.

Therefore, the calibration curves as shown in Figure 4.2.1.D–4.2.1.F were determined in three ranges of absorbed dose.

4.2.2 TLD measurement in Alderson Rando phantom

The TLD measurement in Alderson Rando phantom was performed to measure

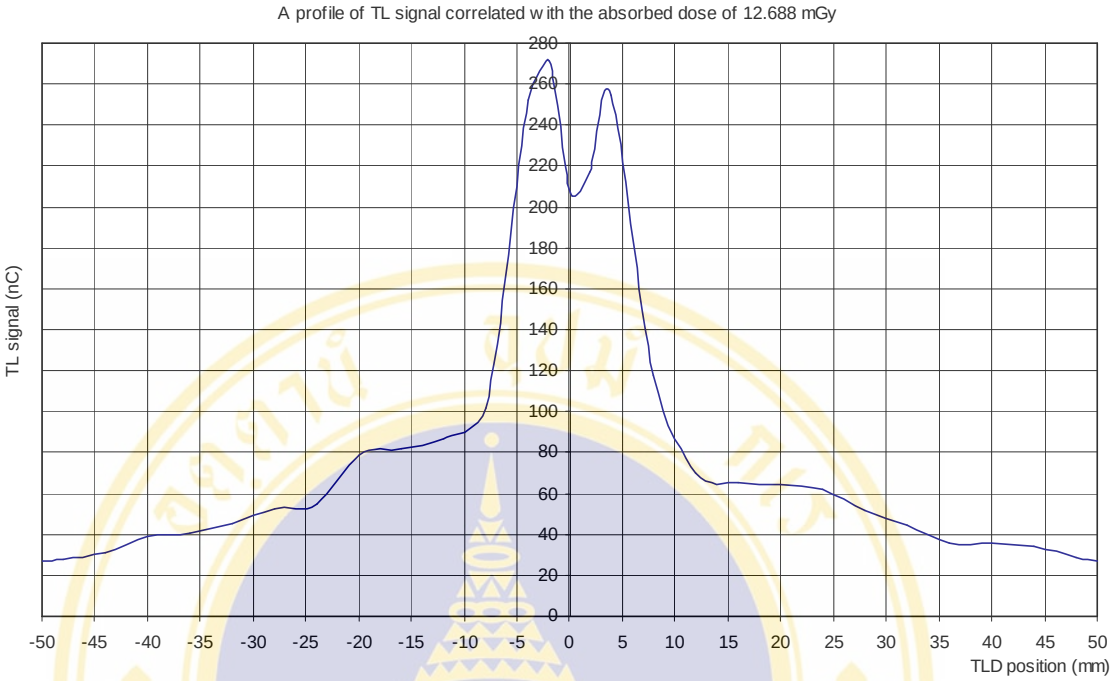

Figure 4.2.1.C A profile of TL signal (nC) correlated with the absorbed dose of 12.688 mGy

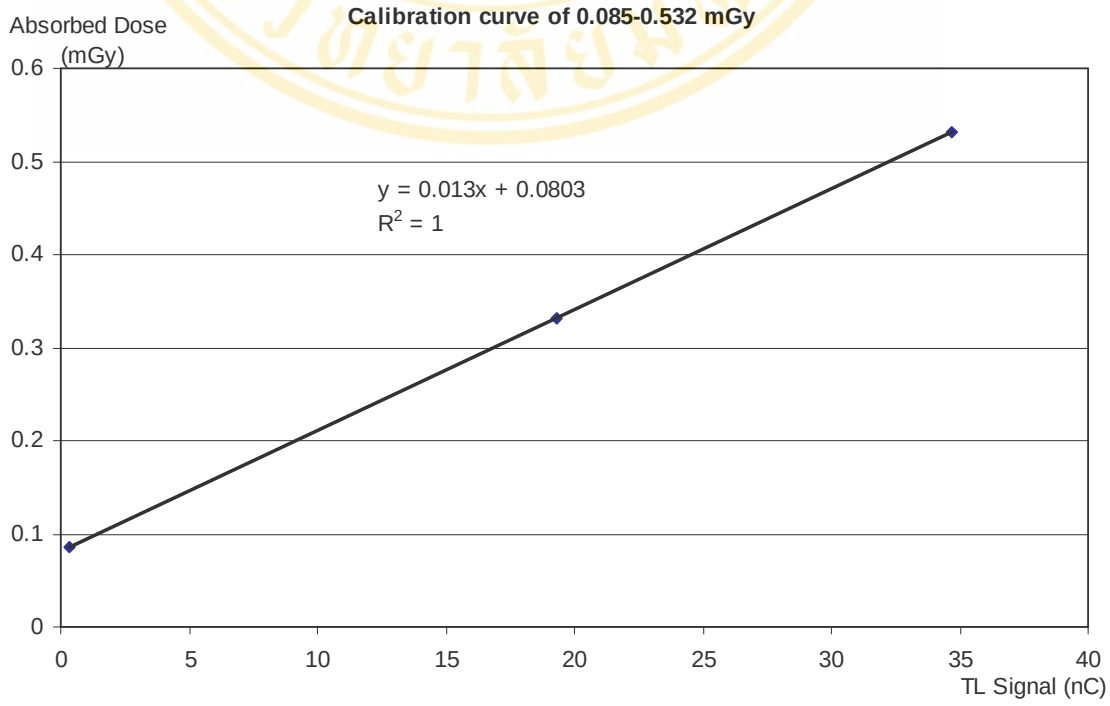

Figure 4.2.1.D Calibration curve ranged in 0.085 – 0.532 mGy

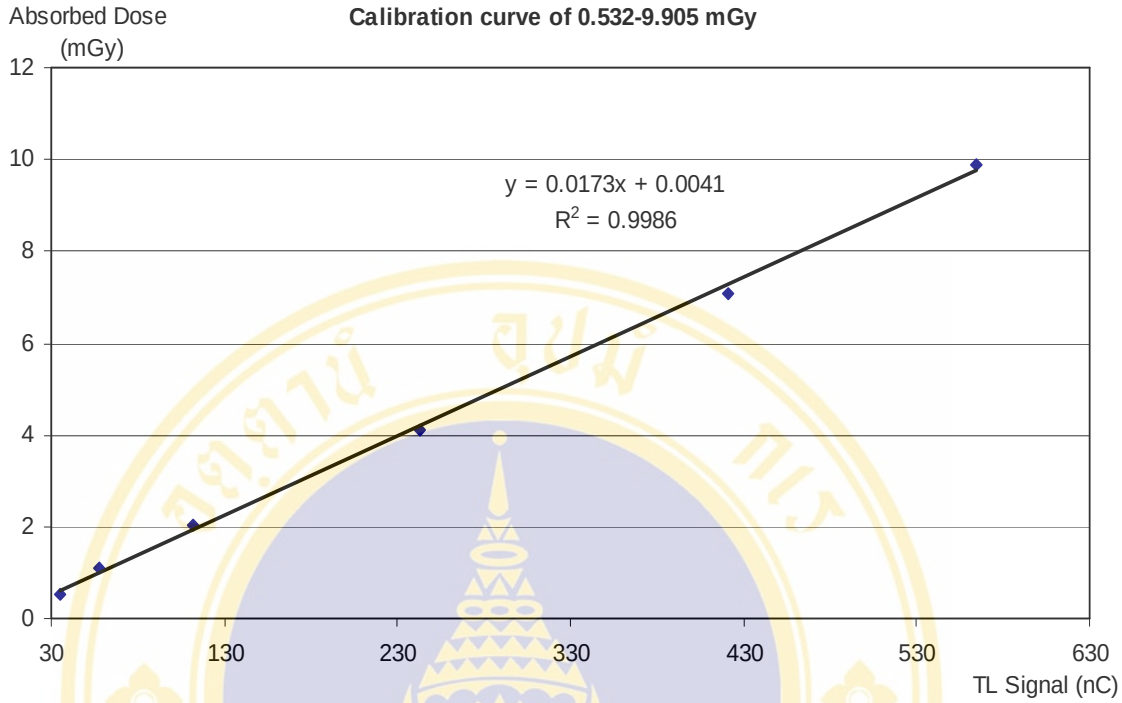

Figure 4.2.1.E Calibration curve ranged in 0.532 – 9.905 mGy

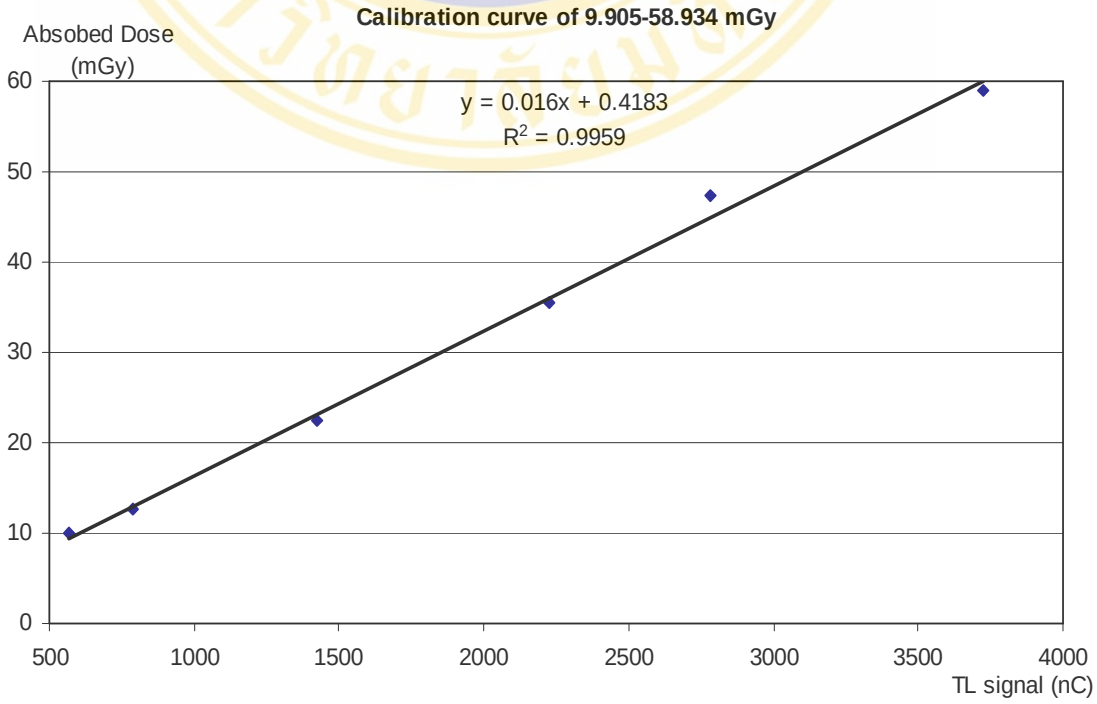

Figure 4.2.1.F Calibration curve ranged in 9.905 -58.934 mGy

the absorbed doses and determined the organ and effective doses in the CT examinations of head, chest, upper abdomen, and lower abdomen as described in the following procedures.

1) The TLDs in Rando phantom plugs were inserted in the organs according to the Recommendation of the International Commission on Radiological Protection (ICRP) Publication 60 (36) as shown in Table 4.2.2.A including eye lens. The organs in each slice of the phantom were located according to Transverse Anatomy of the Human Thorax, Abdomen, and Pelvis: An Atlas of Anatomical Radiological Computed Tomographic and Ultrasonic Correlation (41). The locations of organs and TLDs in each slice are shown in Figure 4.2.2.A.

The remainder organs from the Table 4.2.2.A consist of adrenals, brain, small intestine, kidney, muscle (not calculated in this study), pancreas, spleen, thymus, uterus, and large intestine. A tissue weighting factor of 0.025 was applied to one of the irradiated remainder organ receiving the highest dose in any of these organs and another tissue weighting factor of 0.025 was averaged in the other remainder organs.

Table 4.2.2.A Organs and Tissue weighting factors recommended by the ICRP 60

Tissue or Organs	**Tissue weighting factors (W_T)**
Gonads	0.20
Red bone marrow	0.12
Colon	0.12
Lung	0.12
Stomach	0.12
Bladder	0.05
Breast	0.05
Liver	0.05
Esophagus	0.05

Table 4.2.2.A Organs and Tissue weighting factors recommended by the ICRP 60 (Continued)

Tissue or Organs	Tissue weighting factors (W_T)
Thyroid	0.05
Skin	0.01
Bone surface (skeleton)	0.01
Remainder organs	0.05

2) The Alderson Rando phantom with TLDs was scanned according to the head protocol of GE LightSpeed Plus as shown in Table 4.2.2.B. The head examination is shown in Figure 4.2.2.B.

3) TL signals were read and recorded. Then, the TL signals were multiplied by the correction factor for sensitivity of each TLD shown in Appendix A. The TL signals were averaged in each organ and multiplied by the calibration factors from the calibration curves in section 4.2.1.C to convert these TL signals to the absorbed doses.

4) The effective dose to an organ was calculated by using the following equation.

$$E_T = w_T \bullet w_R \bullet D_{T,R} \qquad \text{Equation 4.2.2}$$

Where E_T is the effective dose to an organ or tissue

w_T is the tissue weighting factor as shown in Table 4.2.2.A

w_R is the radiation weighting factor

$D_{T,R}$ is the average absorbed dose to an organ or tissue

Then, the effective dose in each examination was calculated by a summation of the effective doses to organs recommended by the ICRP 60.

6) All TLDs were annealed. The absorbed doses were measured and the organ and effective doses were determined in the CT examinations of chest, upper abdomen, and lower abdomen according to the TLD measurement in Alderson Rando phantom in section 4.2.2. The scan protocols of these examinations are shown in Table

4.2.2.C-4.2.2.E and the examinations of chest, upper, and lower abdomen are shown in Figure 4.2.2.C-4.2.2.E.

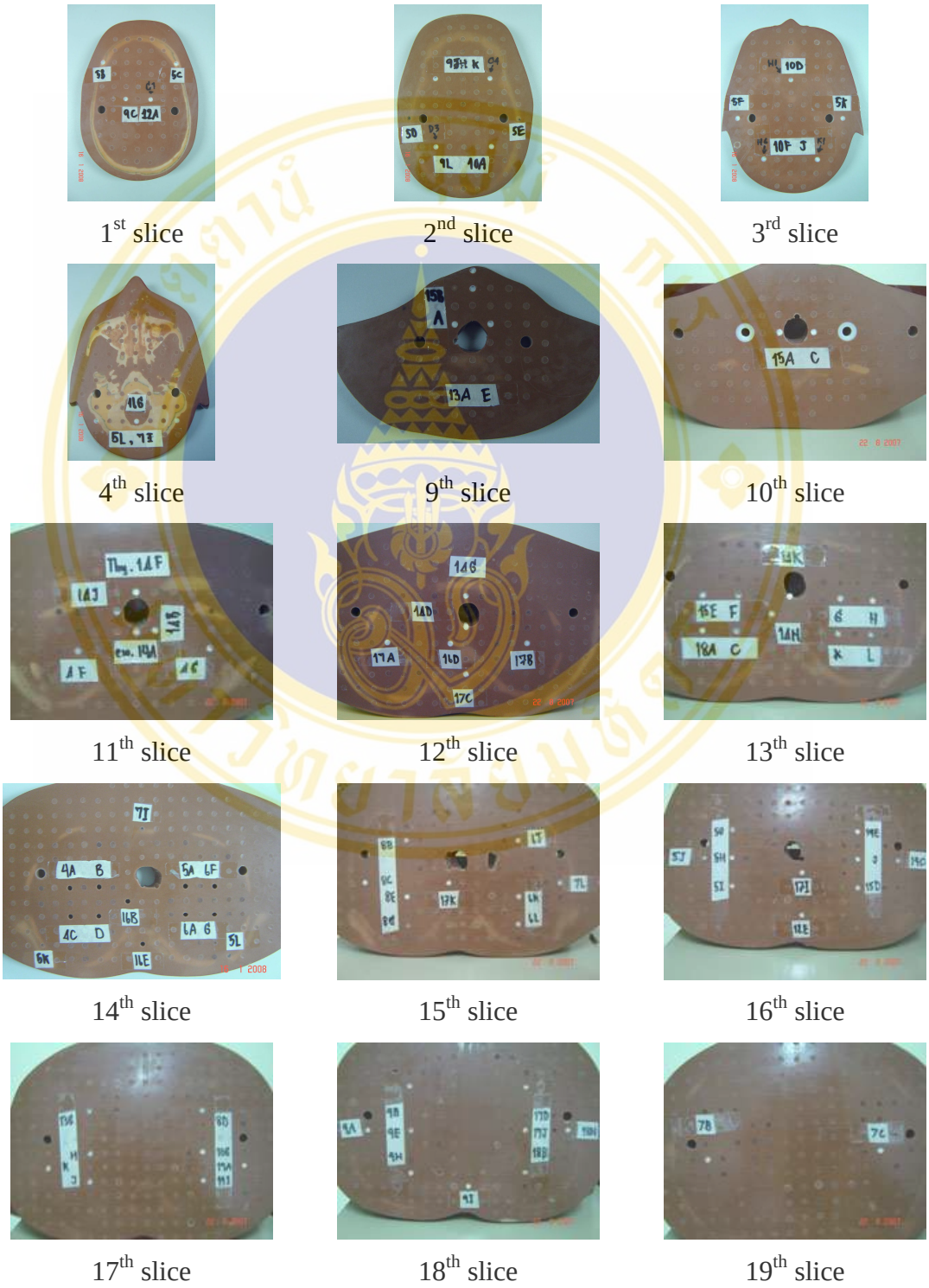

Figure 4.2.2.A Locations of organs and TLDs in each slice

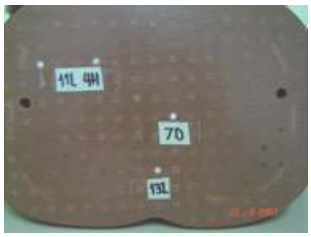

20th slice

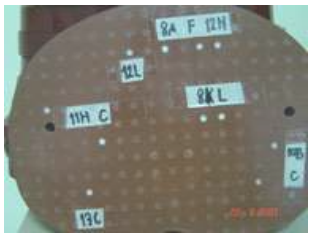

21st slice

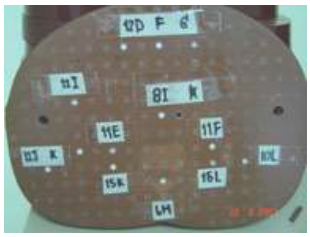

22nd slice

23rd slice

24th slice

25th slice

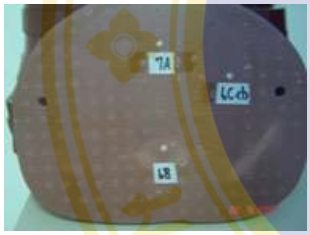

26th slice

27th slice

28th slice

29th slice

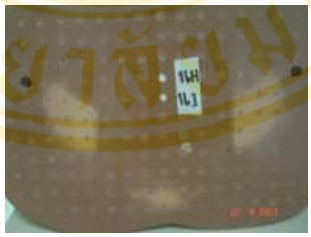

30th slice

31st slice

32nd slice

Figure 4.2.2.A Locations of organs and TLDs in each slice (Continued)

Figure 4.2.2.B Head examination

Table 4.2.2.B Scan protocol of the head examination

Scan protocol of the head examination (1^{st}-4^{th} slice of Rando phantom)		
Scan type	Axial Full 2.0 sec	
Scan section	Base of skull	Base of skull to vertex
Numbers of slices	18	14
Axial thickness (mm)	2.5	5
Numbers of images per rotation	2i	2i
Detector configuration	4 x 1.25	4 x 2.5
Beam collimation (mm)	5.0	10.0
Tube voltage (kV)	120	120
Tube current (mA)	160	140

Table 4.2.2.C Scan protocol of the chest examination

Scan protocol of the chest examination (9^{th}-19^{th} slice of Rando phantom)	
Scan type	Helical Full 0.8 sec
Scan section	Lung apex to base of lung
Numbers of slices	29
Helical thickness (mm)	10
Pitch	0.75 : 1
Speed (mm/rotation)	15.00
Detector configuration	4 x 5.0
Beam collimation (mm)	20.0
Tube voltage (kV)	120
Tube current (mA)	200

Table 4.2.2.D Scan protocol of the upper abdomen examination

Scan protocol of the upper abdomen examination (19^{th}-23^{rd} slice of Rando phantom)	
Scan type	Helical Full 1.0 sec
Scan section	Dome of liver to iliac crest
Numbers of slices	23
Helical thickness (mm)	10
Pitch	0.75 : 1
Speed (mm/rotation)	15.00
Detector configuration	4 x 5.0
Beam collimation (mm)	20.0
Tube voltage (kV)	120
Tube current (mA)	200

Table 4.2.2.E Scan protocol of the lower abdomen examination

Scan protocol of the lower abdomen examination (24^{th}-32^{nd} slice of Rando phantom)	
Scan type	Helical Full 1.0 sec
Scan section	Iliac crest to pelvic floor
Numbers of slices	25
Helical thickness (mm)	10
Pitch	0.75 : 1
Speed (mm/rotation)	15.00
Detector configuration	4 x 5.0
Beam collimation (mm)	20.0
Tube voltage (kV)	120
Tube current (mA)	200

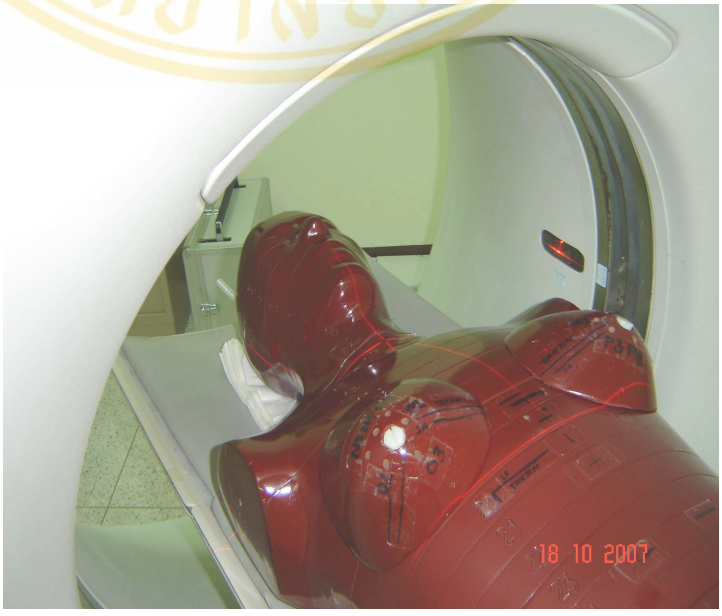

Figure 4.2.2.C Chest examination

Figure 4.2.2.D Upper abdomen examination

Figure 4.2.2.E Lower abdomen examination

4.2.3 Dose calculation by using WinDose® program

In this study, the WinDose® program version 2.1a based on Monte Carlo simulation was used to calculate the organ doses and the effective doses. The input data and parameters required for the WinDose® program are shown in Figure 4.2.3.A.

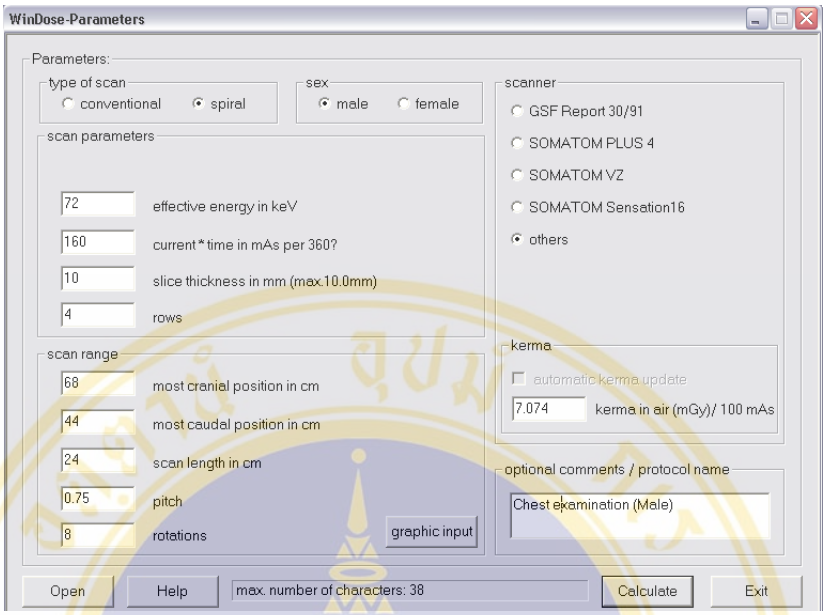

Figure 4.2.3.A WinDose® parameters screen

From the Figure 4.2.3.A, the WinDose® parameters consist of type of scan, scan parameters, scan range, scanner models, and CT air kerma index. From these input data and parameters, effective energy and CT air kerma index free-in-air specific to CT scanner were determined before entering the input data and parameters to the WinDose® program. Therefore, the organ and effective doses calculation by WinDose® program were performed according to these following procedures.

A) Determination of the effective energy

The effective energy of the CT scanner was determined by using the CatPhan® 600 phantom. The determination of the effective energy was described as the following procedures.

1) CatPhan® phantom was set according to the CatPhan® 500 and 600 Manual (40) as shown in Figure 4.2.3.B. The CTP 404 Module of the phantom was scanned with the head protocol described in Table 4.2.2.B using a 10-mm thickness.

2) CT numbers of the seven high contrast sensitometric targets were measured on a CT image of CTP 404 Module shown in Figure 4.2.3.C. The CT numbers of seven high contrast sensitometric targets are shown in Table 4.2.3.A.

3) The effective energy of the CT scanner was determined by a relationship between the CT numbers and linear attenuation coefficients (μ) of the high contrast sensitometric target image shown as the following equation.

$$CT_m = \frac{1000(\mu_m - \mu_w)}{\mu_w} \qquad \text{Equation 4.2.3.A}$$

Where CT_m is the CT number of medium or target image (Houndsfield Units, HU)

μ_m is the linear attenuation coefficient of the medium or target (cm^{-1})

μ_w is the linear attenuation coefficient of water (cm^{-1})

4) To find the linear attenuation coefficient of the sensitometric target, the CT number values of Teflon (958.79 HU), acrylic (120.62 HU), and polystryrene (-37.69 HU) were replaced in the Equation 4.2.3.A. The relationships between the CT numbers and linear attenuation coefficients (μ) of these targets are represented in Equation 4.2.3.B-4.2.3.D.

$$958.79 = \frac{1000(\mu_t - \mu_w)}{\mu_w} \qquad \text{Equation 4.2.3.B}$$

$$120.62 = \frac{1000(\mu_a - \mu_w)}{\mu_w} \qquad \text{Equation 4.2.3.C}$$

$$-37.69 = \frac{1000(\mu_p - \mu_w)}{\mu_w} \qquad \text{Equation 4.2.3.D}$$

5) To find the relationship equation among the linear attenuation coefficients of these targets, the three equations were solved according to Appendix C. Therefore, the relationship equation among the linear attenuation coefficients of the three targets shown in Equation 4.2.3.E was derived.

$$\mu_t = 6.29\,\mu_a - 5.29\,\mu_p \qquad \text{Equation 4.2.3.E}$$

6) The linear attenuation coefficients of acrylic and polystryrene at the corresponding effective energy shown in Table 4.2.3.B were calculated according to the Equation 4.2.3.E to find the correlated values of the linear attenuation coefficient of Teflon.

7) The linear attenuation coefficients of Teflon derived from Equation 4.2.3.E are shown in Table 4.2.3.C. The linear attenuation coefficients were compared with those of Teflon in CatPhan® 600 phantom described in Table 4.2.3.B.

From the table, the minimum of different percentage is 0.903 at 72 keV of the effective energy. Therefore, the effective energy of MDCT scanner is 72 keV.

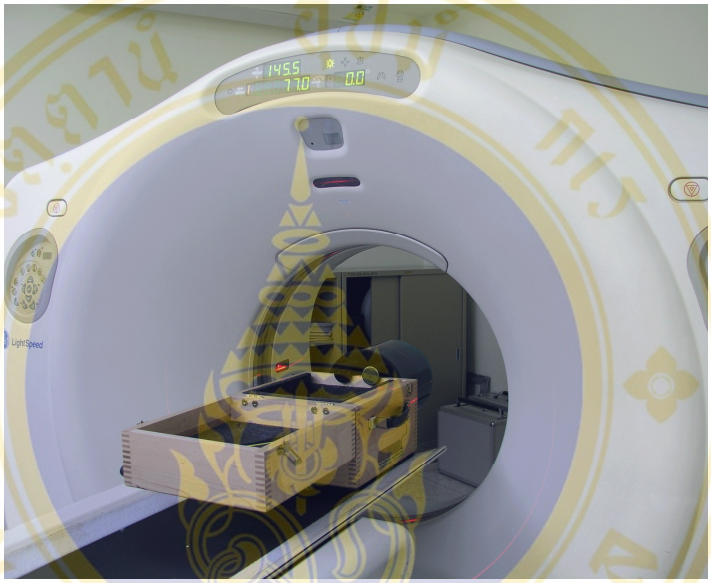

Figure 4.2.3.B CatPhan® 600 phantom set according to the CatPhan® 500 and 600 Manual

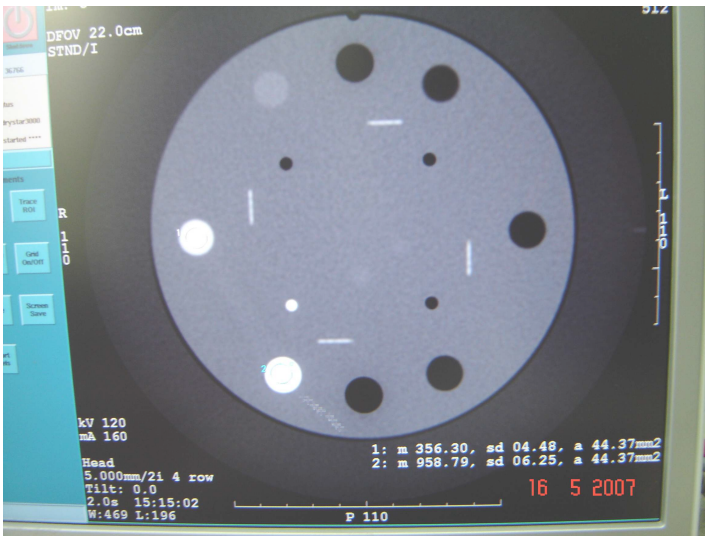

Figure 4.2.3.C CT image of CTP 404 Module of CatPhan® 600 phantom

Table 4.2.3.A CT numbers of the seven high contrast sensitometric targets measured on a CT image of CTP 404 Module

Sensitometric targets	CT numbers (HU)
Teflon	958.79
Delrin	356.30
Acrylic	120.62
Polystrylene	-37.69
Low density polyethylene (LDPE)	-92.90
PMP	-180.73
Air	-972.49

Table 4.2.3.B Linear attenuation coefficients of the targets in CatPhan® 600 phantom at the corresponding effective energy

Effective energy (keV)	Linear attenuation coefficients, μ (cm^{-1})							
	Teflon	Delrin	Acrylic	Polystryrene	Water	LDPE	PMP	Air
64	0.380	0.253	0.221	0.192	0.188	0.178	0.160	0
66	0.374	0.251	0.219	0.191	0.186	0.177	0.160	0
68	0.370	0.248	0.217	0.189	0.184	0.175	0.158	0
70	0.363	0.245	0.215	0.188	0.182	0.174	0.157	0
72	0.359	0.243	0.214	0.186	0.181	0.172	0.155	0
74	0.355	0.240	0.211	0.185	0.179	0.171	0.155	0
76	0.351	0.238	0.210	0.184	0.178	0.170	0.154	0
78	0.346	0.236	0.208	0.183	0.177	0.168	0.152	0
80	0.342	0.234	0.207	0.180	0.175	0.167	0.151	0

Table 4.2.3.C Comparison of the linear attenuation coefficients of Teflon derived from Equation 4.2.3.E and the linear attenuation coefficients of Teflon in CatPhan® 600 phantom

Effective energy (keV)	**Linear attenuation coefficients of Teflon (cm^{-1})**		**Different percentage (%)**
	Derived from equation	**In CatPhan® 600 phantom**	
64	0.380	0.375	1.438
66	0.374	0.367	1.807
68	0.370	0.365	1.286
70	0.363	0.358	1.392
72	0.359	0.362	0.903
74	0.355	0.349	1.788
76	0.351	0.348	0.954
78	0.346	0.340	1.631
80	0.342	0.350	2.324

B) Determination of the CT air kerma index free-in-air

1) The ionization chamber was set to measure the CT air kerma index free-in-air at the central axis of rotation and scanned with a 10 mm thickness with a single rotation and the scan parameters of tube voltage and tube current-time product in each examination as shown in Table 4.2.2.B-4.2.2.E. The absorbed doses were calculated according to the Equation 4.2.2. In the head examination, the CT air kerma index was measured at both 280 mAs and 320 mAs.

2) The CT air kerma index in each examination was calculated to the air kerma index per 100 mAs as shown in Table 4.2.3.D.

C) Dose calculation of the WinDose® program

The input data and parameters as shown in Table 4.2.3.E were entered on

WinDose® parameters screen shown in Figure 4.2.3.A. After clicking Calculate button, the absorbed dose and the effective dose calculated by the WinDose® program were shown in a WinDose® results screen as shown in Figure 4.2.3.D.

Table 4.2.3.D CT air kerma index per 100 mAs in the examinations of head, chest, upper abdomen and lower abdomen

Examinations	**CT air kerma index (mGy)**	**CT air kerma index (mGy) per 100 mAs**
Head - measured at 280 mAs - measured at 320 mAs	 19.737 22.446	 7.049 7.014
Chest	11.319	7.074
Upper abdomen	14.098	7.049
Lower abdomen	14.098	7.049

4.2.4 Data analysis

The organ doses calculated from the WinDose® program were plotted against those determined by the TLD measurement in the examinations of chest, upper abdomen, and lower abdomen. An agreement of the organ doses calculated from the WinDose® program and those resulting from the TLD were found to verify the accuracy of the dose calculation by using the WinDose® program.

In addition, the different percentage of the effective dose in the examinations of head, chest, upper abdomen, and lower abdomen was found from a comparison of the effective doses between the WinDose® calculation and the TLD measurement in all examinations.

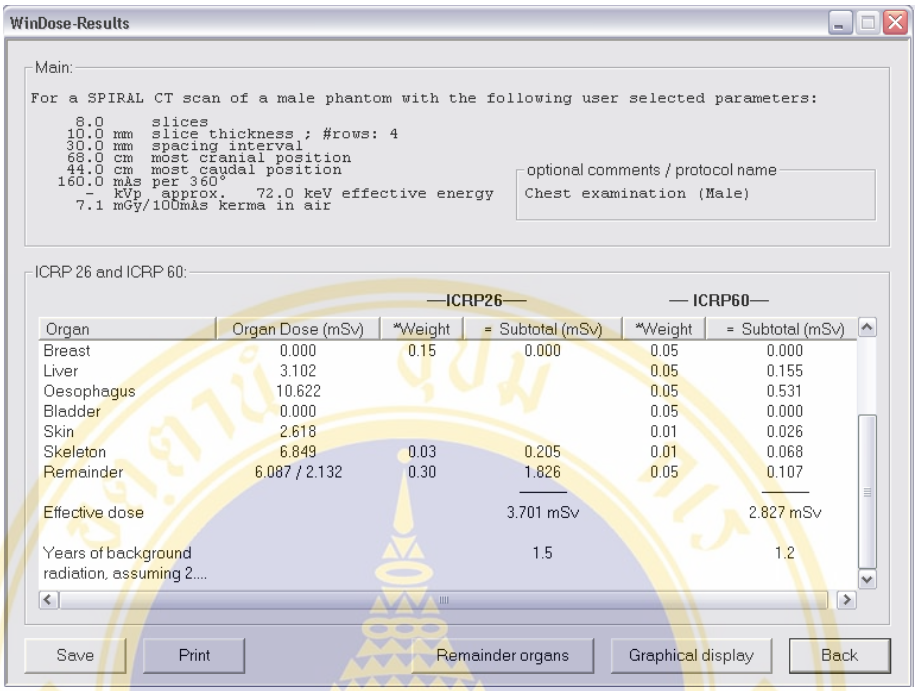

Figure 4.2.3.D WinDose® results screen

Table 4.2.3.E Input data and parameters entered in WinDose® program in the examinations of head, chest, upper abdomen, and lower abdomen

Input data and parameters	**CT examinations**				
	Head		**Chest**	**Upper abdomen**	**Lower abdomen**
Type of scan	Conventional		Spiral	Spiral	Spiral
Scan parameters					
- Effective energy (keV)	72	72	72	72	72
- mAs per 360°	280	320	160	200	200
- Slice thickness (mm)	5	2.5	10	10	10
- Detector rows	4	4	4	4	4
Scan range					
- Most cranial to caudal (cm)	93 - 82	93 - 82	68 - 44	43 - 15	24 - 0
- Scan length (cm)	11	11	24	28	24
- Pitch	1.00	1.00	0.75	0.75	0.75
Air kerma index (mGy)/100 mAs	7.049	7.014	7.074	7.049	7.049

CHAPTER V
RESULTS

5.1 Uncertainty of the absorbed dose measurement by using TLD and the dose calculation by using WinDose® program

The uncertainty of the dose measurement by using TLD and the dose calculation by using the WinDose® program were determined according to the United Kingdom Accreditation Service (UKAS) 2007 (42) and Technical Report series No. 457 from IAEA 2007 (43) and were described in Appendix D. The uncertainty budgets of the dose measurement by using TLD and the dose calculation by using the WinDose® program are shown in Table 5.1.1 and 5.1.2, respectively.

Table 5.1.1 Uncertainty budgets and expanded uncertainty of the absorbed dose measurement using the TLD in Alderson Rando phantom

Uncertainty budgets	Value (%)	Probability distribution	Divisor	Uncertainty (%)
1. TLD grouping	6.7 %	Rectangular	$\sqrt{3}$	3.9 %
2. TLD calibration				
- TLD repeatability	2.5 %	Rectangular	$\sqrt{3}$	1.4 %
- Ionization chamber repeatability	0.4 %	Rectangular	$\sqrt{3}$	0.2 %
3. Calibration factor of ionization chamber (calibration certificate)	5.0 %	Normal	2	2.5 %
4. Measuring accuracy*	6.6 %	Normal	1	6.6 %
Combined uncertainty		**8 %**		
Expanded uncertainty (k = 2)		**16 %**		

* Obtained as a type A which was the maximum standard uncertainty taken from 3 readings at all examinations.

Table 5.1.2 Uncertainty budgets and expanded uncertainty of the dose calculation by using the WinDose® program

Uncertainty budgets	Value (%)	Probability distribution	Divisor	Uncertainty (%)
1. CT air kerma index				
- Ionization chamber repeatability	0.6 %	Normal	1	0.6 %
- Calibration factor of ionization chamber (calibration certificate)	5.0 %	Normal	2	2.5 %
2. Determination of effective energy*	3.0 %	Normal	1	3.0 %
3. WinDose® program	10 %**	Rectangular	$\sqrt{3}$	5.8 %
Combined uncertainty		**7 %**		
Expanded uncertainty (k=2)		**14%**		

* Obtained from repeatability of CatPhan® phantom measurement

** Taken from Zankl M., 1998 (23)

From the Table 5.1.1, the expanded uncertainty of the dose measurement by using TLD is ±16% with 95% confidence limit. From the Table 5.1.2, the expanded uncertainty of the dose calculation by using WinDose® program is ±14% with 95% confidence limit.

5.2 Organ doses in CT examinations

The organ doses resulting from the TLD measurement and the WinDose® calculation are shown in Table 5.2.1 for the head examination and Table 5.2.2 for the examinations of chest, upper abdomen, and lower abdomen. The organ doses are listed according to the organs recommended by the ICRP publication 60. From the Table 5.2.1, the organ dose of uterus in the head examination is lower than the minimum detectable dose of 0.085 mGy. The organ dose calculated from the WinDose® program are shown for both tube current-time products of 280 mAs and 320 mAs. The

hyphen as shown in the Table 5.2.1 and the Table 5.2.2 represents the organ doses of 0.000 mGy resulting from the WinDose® calculation.

Table 5.2.1 Organ doses in mGy resulting from TLD measurement and WinDose® calculation in the head examination

Organs	Absorbed doses (mGy)		
	TLD measurement	WinDose® calculation	
		280 mAs	320 mAs
Gonads	0.342	-	-
Red bone marrow	10.412	2.849	1.620
Colon	0.362	-	-
Lung	0.818	0.027	0.015
Stomach	0.705	-	-
Bladder	0.357	-	-
Breast	1.535	-	-
Liver	0.743	-	-
Esophagus	3.755	0.026	0.015
Thyroid	0.270	0.724	0.412
Skin	11.651	1.154	0.877
Bone surface	19.137	6.631	3.770
Adrenals	0.553	-	-
Brain	15.814	22.917	13.031
Small intestine	0.467	-	-
Kidney	0.521	-	-
Pancreas	0.768	-	-
Spleen	1.392	-	-
Large intestine	0.470	-	-
Uterus	< 0.085	-	-
Thymus	6.715	0.026	0.015
Eye lens	2.139	31.101	17.684

Table 5.2.2 Organ doses in mGy resulting from TLD measurement and WinDose® calculation in the examinations of chest, upper abdomen, and lower abdomen

Organs	Absorbed dose (mGy)					
	Chest		Upper abdomen		Lower abdomen	
	TLD	WinDose	TLD	WinDose	TLD	WinDose
Gonads	0.096	-	0.189	0.169	12.171	10.878
Red bone marrow	8.451	2.406	5.798	3.890	9.471	3.796
Colon	0.187	0.010	9.958	5.123	11.417	9.687
Lung	10.181	10.957	2.529	2.709	0.149	0.033
Stomach	7.532	1.879	12.748	11.982	0.536	0.870
Bladder	0.112	-	1.011	2.590	10.049	11.410
Breast	8.128	11.628	3.727	1.880	0.231	0.030
Liver	8.467	3.102	11.668	11.278	0.424	0.628
Esophagus	8.525	10.622	0.659	0.326	0.108	0.004
Thyroid	2.734	2.192	0.148	0.034	0.106	-
Skin	10.924	2.618	13.183	3.434	12.395	3.165
Bone surface	9.518	6.849	11.776	6.613	9.930	4.865
Adrenals	3.393	3.471	9.542	9.261	0.795	0.209
Brain	0.208	0.102	0.092	-	0.091	-
Small intestine	0.869	0.083	14.499	10.201	6.369	8.501
Kidney	3.000	0.576	11.238	12.426	1.337	1.058
Pancreas	6.528	2.028	10.484	9.618	0.500	0.458
Spleen	6.905	2.204	10.552	11.769	0.373	0.464
Large intestine	0.740	0.104	13.210	10.791	4.424	8.767
Uterus	0.126	0.017	1.705	7.935	9.641	9.959
Thymus	9.941	10.622	0.295	0.326	0.100	0.004
Eye lens	0.255	0.130	0.113	-	0.104	-

The comparisons of organ doses between the TLD measurement and the WinDose® calculation in the examinations of chest, upper abdomen, and lower abdomen are shown in Figure 5.2.1 for the doses in scan sections and Figure 5.2.2 for the doses outside scan sections.

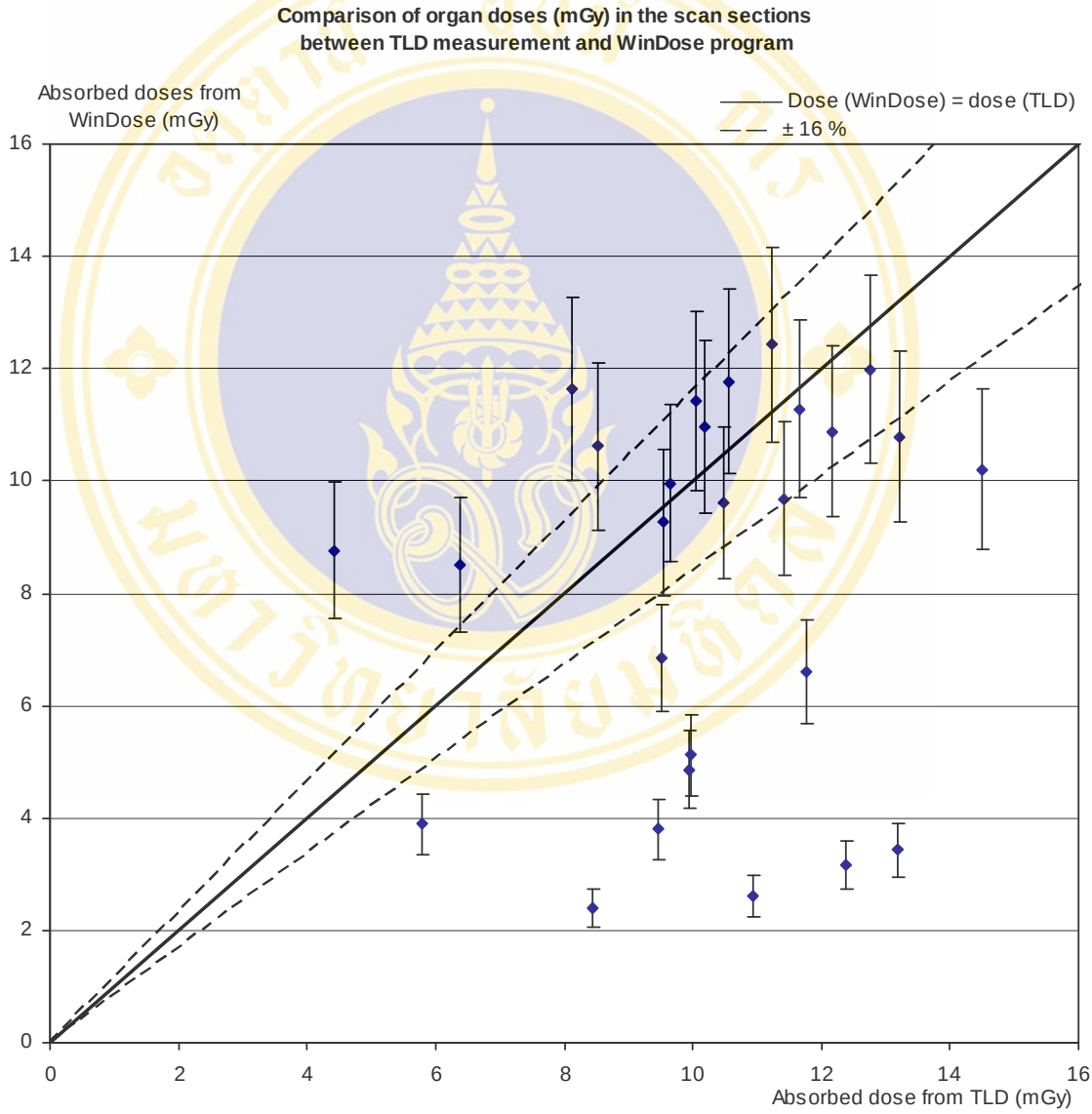

Figure 5.2.1 Comparison of organ doses (mGy) in the scan sections between TLD measurement and WinDose® program in the examinations of chest, upper abdomen, and lower abdomen. The error bars show the uncertainty of dose calculation by using the WinDose® program with ±14%.

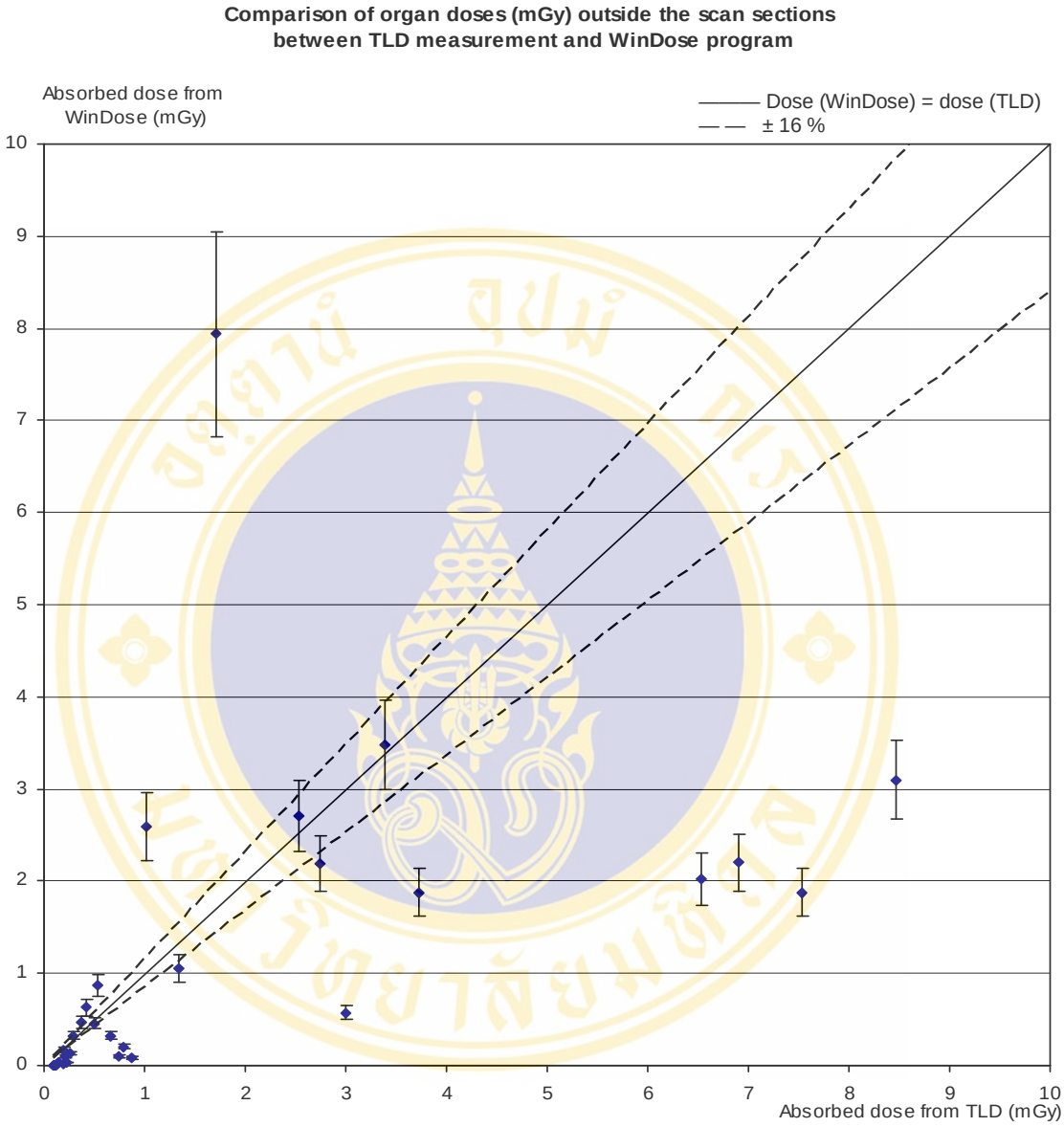

Figure 5.2.2 Comparison of organ doses (mGy) outside the scan sections between TLD measurement and WinDose® program in the examinations of chest, upper abdomen, and lower abdomen. The error bars show the uncertainty of dose calculation by using the WinDose® program with ±14%. The organ doses of 0.000 mGy calculated from the WinDose® program are not included.

From the Figure 5.2.1 and the Figure 5.2.2, the solid line represents the values of organ dose resulting from the WinDose® calculation equal to those from the TLD measurement. The upper dash line and the lower dash line indicate the values of

organ dose calculated from WinDose® program with 16% higher and 16% lower than those determined by the TLD measurement, respectively. The organ doses resulting from both methods in the head examination are not included because of the differences in their scan parameters.

The comparison of organ doses in the scan sections between the TLD measurement and the WinDose® calculation in the examinations of chest, upper abdomen, and lower abdomen showed an agreement within ±16% corresponding to the uncertainty of the absorbed dose measurement by using the TLD in Alderson Rando phantom, except for the organ doses of breast in the chest examination, some extended organs in the examinations of upper abdomen and lower abdomen, red bone marrow, skin, and bone surface in the three examinations as shown in Table 5.2.3.

Table 5.2.3 Organ doses of breast in the chest examination, the extended organs in the examinations of upper abdomen and lower abdomen, red bone marrow, skin, bone surface in the examinations of chest, upper abdomen and lower abdomen

Examinations	**Organs**	**Absorbed doses (mGy)**	
		TLD	**WinDose® program**
Chest	Red bone marrow	8.451	2.406
	Skin	10.924	2.618
	Bone surface	9.518	6.849
	Breast	8.128	11.628
Upper abdomen	Red bone marrow	5.798	3.890
	Skin	13.183	3.434
	Bone surface	11.776	6.613
	Colon	9.958	5.123
	Small intestine	14.499	10.201
Lower abdomen	Red bone marrow	9.471	3.763
	Skin	12.395	3.165
	Bone surface	9.930	4.865
	Large intestine	4.424	8.767

From the comparison of organ doses outside the scan sections between the TLD measurement and the WinDose® calculation in the examinations of chest, upper abdomen, and lower abdomen, the doses calculated from the WinDose® program tend to be lower than those determined by the TLD measurement especially stomach, liver, pancreas, and spleen in the chest examination. However, the organ doses of bladder and uterus in the upper abdomen examination, stomach and liver in the lower abdomen examination resulting from the WinDose® calculation are higher than those from the TLD measurement. The organ doses of stomach and liver are shown in Figure 5.2.3 which represents the organ doses outside the scan sections less than 1.000 mGy.

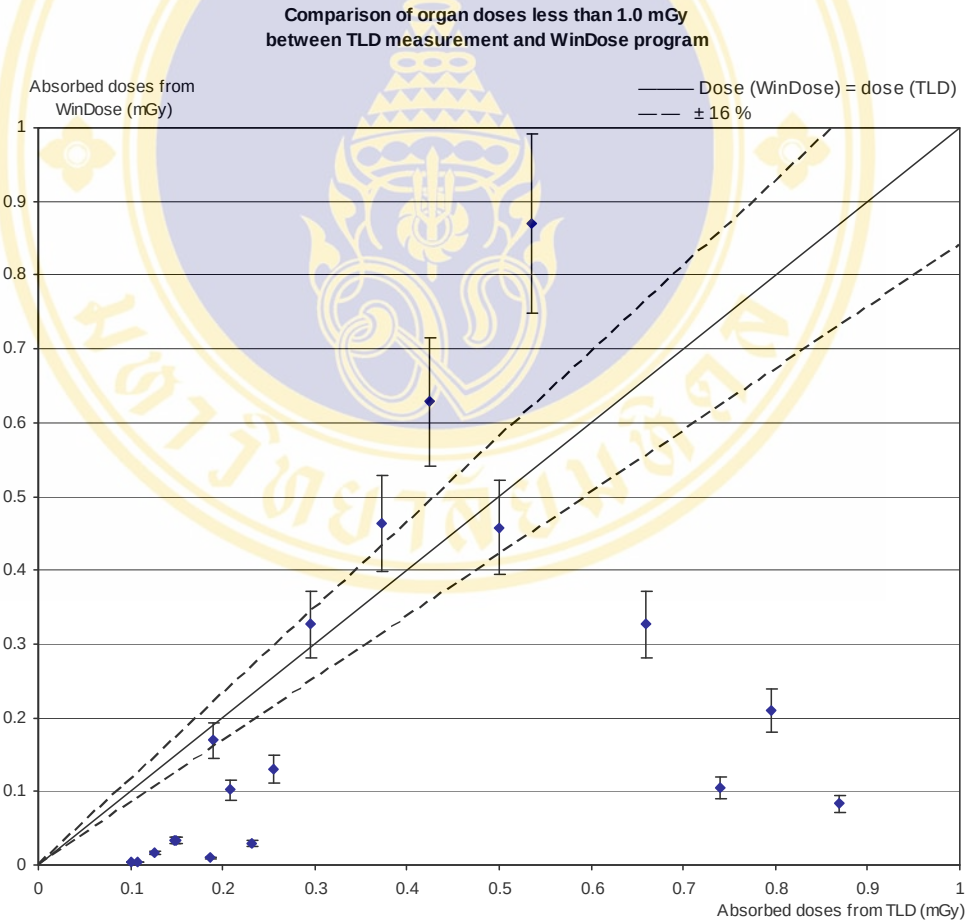

Figure 5.2.3 Comparison of organ doses (mGy) outside the scan sections between TLD measurement and WinDose® program less than 1.000 mGy in the examinations of chest, upper abdomen, and lower abdomen. The error bars show the uncertainty of dose calculation by using the WinDose® program with ±14%.

5.3 Effective doses to organs in CT examinations

Details of effective doses to organs resulting from the TLD and the WinDose® program are shown in Table 5.3.1 for the head examination and Table 5.3.2. for the examinations of chest, upper and lower abdomen. The effective doses are listed according to radiosensitivity of organs recommended by the ICRP 60. From the tables, large contributors to effective doses resulting from both methods are red bone marrow and bone surface in the head examination, lung in the chest examination, stomach and colon in the upper abdomen examination, gonad and colon in the lower abdomen examination. The hyphen represents the effective doses to organs of 0.000 mSv.

Table 5.3.1 Details of the effective doses to organs (mSv) contributing to the effective doses resulting from TLD measurement and WinDose® calculation in the head examination

Organs	Effective doses to organs (mSv)		
	TLD measurement	WinDose® calculation	
		280 mAs	320 mAs
Gonads	0.068	-	-
Red bone marrow	1.249	0.342	0.194
Colon	0.043	-	-
Lung	0.098	0.003	0.002
Stomach	0.085	-	-
Bladder	0.018	-	-
Breast	0.077	-	-
Liver	0.037	-	-
Esophagus	0.188	0.001	0.001
Thyroid	0.014	0.036	0.021
Skin	0.117	0.015	0.009
Bone surface	0.191	0.066	0.038
Remainder organs	0.506	0.573	0.326
Effective dose (mSv)	**2.691**	**1.037**	**0.591**

Table 5.3.2 Details of the effective doses to organs (mSv) contributing to the effective doses resulting from TLD measurement and WinDose® calculation in the examinations of chest, upper abdomen, and lower abdomen

Organs	Effective doses to organs (mSv)					
	Chest		Upper abdomen		Lower abdomen	
	TLD	WinDose	TLD	WinDose	TLD	WinDose
Gonads	0.019	-	0.038	0.034	2.434	2.176
Red bone marrow	1.014	0.289	0.696	0.467	1.137	0.456
Colon	0.022	0.001	1.195	0.615	1.370	1.162
Lung	1.222	1.315	0.303	0.325	0.018	0.004
Stomach	0.904	0.225	1.530	1.438	0.064	0.104
Bladder	0.006	-	0.051	0.129	0.502	0.570
Breast	0.406	0.581	0.186	0.094	0.012	0.002
Liver	0.423	0.155	0.583	0.564	0.021	0.031
Esophagus	0.426	0.531	0.033	0.016	0.005	-
Thyroid	0.137	0.110	0.007	0.002	0.005	-
Skin	0.109	0.026	0.132	0.034	0.124	0.032
Bone surface	0.095	0.068	0.118	0.066	0.099	0.049
Remainder organs	0.317	0.107	0.566	0.473	0.291	0.108
Effective dose (mSv)	**5.100**	**3.408**	**5.438**	**4.282**	**6.082**	**4.749**

5.4 Effective dose in CT examinations

The effective doses resulting from the TLD measurement and the WinDose® calculation in the examinations of head, chest, upper abdomen, and lower abdomen are shown in Table 5.4. From the table, the effective doses calculated from the WinDose® program are 61% and 78%, 33%, 21%, and 22% lower than those from the TLD measurement in the examinations of head, chest, upper abdomen, and lower abdomen, respectively.

Table 5.4 Comparison of the effective doses between the TLD measurement and the WinDose® program in the examinations of head, chest, upper abdomen, and lower abdomen

Examinations	**Effective dose (mSv)**		**Different percentages**
	TLD measurement	**WinDose® program**	
Head	2.69*	1.04** 0.59***	61% 78%
Chest	5.10	3.41	33%
Upper Abdomen	5.44	4.28	21%
Lower Abdomen	6.08	4.75	22%

*Scanned with the tube current-time products of 280 and 320 mAs

** Scanned with the tube current-time products of 280 mAs

*** Scanned with the tube current-time products of 320 mAs

CHAPTER VI
DISCUSSION

6.1 Organ doses in the CT examinations

The comparison of organ doses in the scan sections between the TLD measurement and the WinDose® calculation in the examinations of chest, upper abdomen, and lower abdomen showed an agreement within ±16% which was the uncertainty of the dose measurement by using TLD in Alderson Rando phantom. However, the organ doses of small intestine and colon calculated from the WinDose® program were lower than those from the TLD in the upper abdomen examination, and also the organ doses of large intestine from the WinDose® were higher than those from the TLD in the lower abdomen examination. These deviations would be due to the differences in the organ length of these extended organs. Most length of the small and large intestine in the Alderson Rando phantom was located in the upper abdomen whereas those in the mathematical phantom were located in the lower abdomen, and also the length of colon in the upper abdomen in the mathematical phantom was less than that in the Rando phantom.

The organ dose of breast in the chest examination calculated from the WinDose® was overestimated because its organ dose conversion coefficients would not be taken into account the fractions of the organ volume directly irradiated. The same result found by Geleijns et al., 1994 (18) which the organ dose of breast calculated from the CTDI combined with organ dose conversion coefficients was approximately 40% higher than that determined by the TLD in the thorax examination.

The organ doses of red bone marrow, skin, and bone surface calculated from the WinDose® program were less than those from the TLD due to the differences in determination of organ length in both methods. The organ doses of red bone marrow, skin, and bone surface resulting from the TLD measurement were measured in the scan section of each examination whereas those organ doses resulting from the mathematical phantom.

From the comparisons of organ doses outside the scan sections between the TLD measurement and the WinDose® program in the examinations of chest, upper abdomen, and lower abdomen shown in Figure 5.2.2, the doses from the WinDose® calculation were lower than those from the TLD measurement in the three examinations, especially stomach, liver, pancreas, and spleen in the chest examination. The lower organ doses calculated from the WinDose® program could be the results from the scattered radiation not taken into account for organs further away from the scan sections.

The lower doses of stomach, liver, pancreas, and spleen in the chest examination could be also due to more realistic distribution of these organs in the Alderson Rando phantom than the mathematical phantom. In Rando phantom, some parts of the stomach, liver, pancreas, and spleen were located in the lower part of the lung whereas these organs were sharp boundary and separately located from the lower part of the lung in the mathematical phantom. This result was also found by Geleijns et al., 1994 (18) in the thorax examination.

However, in the upper abdomen examination, the organ doses of bladder and uterus from the WinDose® calculation were up to 100% higher than those from the TLD. The higher doses would be due to the difference in the organ locations between the Alderson Rando phantom and the mathematical phantom. For example, the uterus in the Rando phantom was located lower than the scan section of upper abdomen examination whereas the uterus in the mathematical phantom was located at the edge of scan section. Zankl M., 1998 (23) also mentioned this deviation of organ doses of small organs located at the edge of the radiation field.

6.2 Effective doses to organs in the CT examination

From the details of effective doses to organs resulting from the TLD measurement and the WinDose® program in the examinations of head, chest, upper abdomen, and lower abdomen, the large contributors to effective dose resulting from both methods were red bone marrow and bone surface in the head examination, lung in the chest examination, stomach and colon in the upper abdomen examination, gonad and colon in the lower abdomen examination. From Peter F., 2001 (37), the largest contributors to effective dose calculated by EGS4-VLSI code based on Monte Carlo simulation

showed the similar results in the examinations of head and upper abdomen.

6.3 Effective doses in the CT examinations

The effective doses calculated from the WinDose® program were lower than those determined by the TLD in ranges of 21-33% except for the head examination which was more than 60%. The similar figures were found by Geleijns et al., 1994 (18) and Groves et al., 2004 (21) which the effective doses calculated from the CTDI and the organ dose conversion coefficients were up to 40% and 18%, respectively, lower than those resulting from the TLD measurement.

Comparison of the effective doses with the previous studies in the examinations of head, chest, upper abdomen and lower abdomen are shown in Table 6.3.1-6.3.4. The effective doses were normalized to the effective doses in mSv per 100 mAs with the pitch equal to 1 and were not taken into account the effect of beam collimation between the scan parameters in each study. In general, the effective doses resulting from the calculation based on Monte Carlo simulation are less than those determined by the TLD measurement in the examinations of head, chest, upper abdomen, and lower abdomen. The effective doses in this study are lower dose as comparison with some studies because of the differences in their scanner geometry, beam quality, including the scanning parameters in each examination. However, the effective doses resulting from the TLD measurement and the WinDose® calculation in the examinations of head, chest, upper abdomen, and lower abdomen are in a range of typical effective dose values reported by AAPM Report No. 96 (1).

In the head examination, the effective doses resulting from WinDose® calculation were 61% and 78% lower than those from the TLD measurement for 280 and 320 mAs, respectively, because of various scan sections in this examination. The TLD measurement in Alderson Rando phantom was performed with the scan protocol consisting of the two sets of slice thickness and scan section which are the 2.5 mm thickness at base of skull and the 5 mm thickness above base of skull as shown in Table 4.2.2.B. Each set of slice thickness and scan section was scanned with different tube current-time products which were 320 mAs at base of skull and 280 mAs above base of skull whereas the WinDose® calculation was entered the only value of slice thickness, scan section, and scan parameter per a calculation. This result may suggest

that the WinDose® program can not be used to calculate the organ doses and the effective dose in the head examination with the various scan sections.

Table 6.3.1 Comparison of the effective doses (mSv) per 100 mAs in the head examination with the previous studies

Studies / CT scanners	**Scan parameters**					**Effective doses (mSv) per 100 mAs**	
	Tube voltage (kV)	Tube current-time product (mAs)	Beam collimation (mm)	Pitch	Scan length (cm)	TLD measurement	WinDose program or Monte Carlo calculation
This study	120	320 and 280	5 and 10	1.00	12 / 11*	0.96**	0.37**
Geleijns et al.	120	363	10	1.00	12	0.52	0.58 (CTDI with GSF) 0.41 (CTDI with NRPB)
Hidajat et al.	120	250	10	1.00	16	-	0.40
Peter F.	120	390	10	1.00	14	-	0.19
Brix et al. - GE Lightspeed QX/i	120	200	20 (4x5 mm)	0.75	15	0.75***	0.71***
- Philips Mx8000 Quad	120	219	10 (4x1.25 mm)	0.875	15	0.60***	0.52***
Van der Molen et al.	120	200	10 (16x0.625mm)	0.5625	14	-	1.15

* Scan length of the Alderson Rando phantom / scan length of the mathematical phantom

** Normalized from 280 mAs

*** Normalized to the pitch equal to 1.00

Table 6.3.2 Comparison of the effective doses (mSv) per 100 mAs in the chest examination with the previous studies

Studies / CT scanners	**Scan parameters**					**Effective doses (mSv) per 100 mAs**	
	Tube voltage (kV)	Tube current-time product (mAs)	Beam collimation (mm)	Pitch	Scan length (cm)	TLD measurement	WinDose program or Monte Carlo calculation
This study	120	160	20	0.75	28 / 24*	1.91**	1.28**
Geleijns et al.	120	333	10	1.00	27	5.41	4.51 (CTDI with GSF) 3.30 (CTDI with NRPB)
Hidajat et al.	137	180	10	1.00	24	-	2.98
Peter F.	-	-	-	-	-	-	-
Brix et al.							
- GE Lightspeed QX/i	120	104	20 (4x5 mm)	1.50	27.8	5.48**	4.04**
- Philips Mx8000 Quad	120	87.5	10 (4x2.5 mm)	0.875	27.3	3.90**	3.10**
Van der Molen et al.	120	120	20 (16x1.25mm)	1.375	27	-	4.70**

* Scan length of the Alderson Rando phantom / scan length of the mathematical phantom

** Normalized to the pitch equal to 1.00

Table 6.3.3 Comparison of the effective doses (mSv) per 100 mAs in the upper abdomen examination with the previous studies

Studies / CT scanners	**Scan parameters**					**Effective doses (mSv) per 100 mAs**	
	Tube voltage (kV)	Tube current-time product (mAs)	Beam collimation (mm)	Pitch	Scan length (cm)	TLD measurement	WinDose program or Monte Carlo calculation
This study	120	200	20	0.75	22 / 28*	2.04**	1.61**
Geleijns et al.	120	380	10	1.00	30	6.32	5.26 (CTDI with GSF) 3.95 (CTDI with NRPB)
Peter F.	120	200	10	1.00	19	-	1.78 - 2.06
Hidajat et al.	120	210	10	1.00	15	-	1.77
Brix et al.	-	-	-	-	-	-	-
Van der Molen et al.***	120	150	20 (16x1.25mm)	1.375	42	-	7.15**

* Scan length of the Alderson Rando phantom / scan length of the mathematical phantom

** Normalized to the pitch equal to 1.00

*** Whole abdomen

Table 6.3.4 Comparison of the effective doses (mSv) per 100 mAs in the lower abdomen examination with the previous studies

Studies / CT scanners	Scan parameters					Effective doses (mSv) per 100 mAs	
	Tube voltage (kV)	Tube current-time product (mAs)	Beam collimation (mm)	Pitch	Scan length (cm)	TLD measurement	WinDose program or Monte Carlo calculation
This study	120	200	20	0.75	24 / 23*	2.28**	1.78**
Geleijns et al.	-	-	-	-	-	-	-
Hidajat et al.***	120	210	10	1.00	26	-	2.61
Peter F.	-	-	-	-	-	-	-
Brix et al.***							
- GE Lightspeed QX/i	120	200	20 (4x5 mm)	1.5	19.5	4.13**	3.53**
- Philips Mx8000 Quad	120	225	20 (4x5 mm)	0.625	26.3	4.33**	3.56**
Van der Molen et al.	-	-	-	-	-	-	-

* Scan length of the Alderson Rando phantom / scan length of the mathematical phantom

** Normalized to the pitch equal to 1.00

*** Pelvis examination

CHAPTER VII
CONCLUSION

The WinDose® program version 2.1a can be used to calculate the organ doses and the effective doses in the examinations of chest, upper abdomen, and lower abdomen. The organ doses in the scan sections calculated from the WinDose® program are accurate within ±16%. In the scan sections, the calculation of organ doses by using the WinDose® program should be aware of underestimation of the organ doses of colon and small intestine in the upper abdomen examination and overestimation of the organ doses of large intestine in the lower abdomen examination. The organ dose of breast in the chest examination calculated from the WinDose® program will be overestimated more than 16% as compared to that determined by the TLD measurement.

The organ doses outside the scan sections calculated from the WinDose® program are lower than those determined by the TLD measurement, especially stomach, liver, pancreas, and spleen in the chest examination including the organs located far away from the scan sections. The organ doses of stomach, liver, pancreas, and spleen located in the lower part of the lung from the WinDose® calculation are lower than those resulting from the TLD in ranges of 63-75%. However, the calculation of organ doses by using the WinDose® program should be aware of the overestimation of organ doses of bladder and uterus in the upper abdomen examination.

The effective doses in the CT examinations calculated from the WinDose® program are less than those determined by the TLD measurement in Alderson Rando phantom in range of 21-33%. The head examination or the examinations consisting of the various scan sections with different scan parameters should be separately calculated.

REFERENCES

1. American Association of Physicists in Medicine (AAPM). The Measurement, Reporting, and Management of Radiation Dose in CT. AAPM Report No. 96. AAPM; 2008.
2. Jessen KA, Shrimpton PC, Geleijns J, Panzer W, Tosi G. Dosimetry for optimization of patient protection in computed tomography. Appl Radiat Isot 1999; 50: 165-72.
3. Shrimpton PC, Wall BF. The increasing importance of x ray computed tomography as a source of medical exposure. Radiat Prot Dosimetry 1995; 57: 413-5.
4. Poletti JL. Patient doses from CT in New Zealand and a simple method for estimating effective dose. Br J Radiol 1996 May; 69(821): 432-6.
5. Kual A, Bauer B, Bernhardt J, Nosske D, Veit R. Effective doses to members of the public from the diagnostic application of ionizing radiation in Germany. Eur J Radiol 1997; 7: 1127-32.
6. Hart D, Wall BF. UK population dose from medical X-ray examinations. Eur J Radiol 2004; 50: 285-91.
7. Shrimpton PC, Hiller MC, Lewis MA, Dunn . National survey of doses from CT in the UK: 2003. Br J Radiol 2006; 79: 968-80.
8. Brix G, Nagel HD, Stamm G, Veit R, Lechel U, Griebel J, Galanski M, Radiation exposure in multi-slice versus single-slice spiral CT: results of a nationwide survey. Eur J Radiol 2003; 13: 1979-91.
9. McCollough CH, Schueler BA. Education Treatise: Calculation of effective dose. Med Phys 2000 May; 27(5): 828-37.
10. International Commission on Radiation Units and Measurements (ICRU). Patient dosimetry for x rays used in medical imaging. Methods for determining organ and tissue doses. ICRU Report No. 74. Journal of ICRU 2005; 5(2): 55-62.
11. Martin CJ. Effective dose: how should it be applied to medical exposures. Health

Phys 2007; 80: 639-47.

12. Michael F. Radiation dose in CT. Radiographics 2002; 22: 1541-53.
13. International Commission on Radiation Units and Measurements (ICRU). Patient dosimetry for x rays used in medical imaging. Quantities and units for measurement and calculation in medical x-ray imaging. ICRU Report No. 74. Journal of ICRU 2005; 5(2): 25-34.
14. American Association of Physicists in Medicine (AAPM). Standardized Methods for Measuring Diagnostic X-Ray Exposures. AAPM Report No. 31. New York: AAPM; 1990.
15. Edward CR, Mountford PJ, Green S, Palethorpe JE, Moloney AJ. The low energy x-ray response of the LiF: Mg: Cu: P thermoluminescent dosemeter: a comparison with LiF: Mg: Ti. Br J Radiol 2005; 78: 543-47.
16. Karl KL. Investigation of dosimetric characteristics of the high sensitivity LiF: Mg, Cu, P Thermoluminescent Dosemeter and its applications in diagnostic radiology—a review. Radiography 2004; 10: 145-50.
17. Ziying Z, Shoushan W, Fang W, Guolong C, Yaunfang Z, Jianhuan Z. Measurement of extremely low level dose with LiF (Mg, Cu, P) TL chips. Radiat. Prot. Dosimetry 1986; 17: 415-8.
18. Geleijns J, Van Unnik JG, Zoetelief J, Zweers D, Broerse JJ. Comparison of two methods for assessing patient dose from computed tomography. Br J Radiol 1994 Apr; 67: 360-5.
19. Adams EJ, Brettle DS, Jones AP, Hounsell AR, Mott DJ. Estimation of fetal and effective dose for CT examinations. Br J Radiol 1997 Mar; 70: 272-278.
20. Alonso M, Barriuso T, Castaneda MJ, Diaz-Caneja N, Gutierrez I, Villar E. Monte Carlo estimation of absorbed dose to organs in computed tomography. Health Phys 2002; 82(2): 233-9.
21. Groves AM, Owen KE, Courtney HM, Yates SJ, Goldstone KE, Blake GM, et al. 16-detector multislice: dosimetry estimation by TLD measurement compared with Monte Carlo Simulation. Br J Radiol 2004 Aug; 77: 662-5.
22. Brix G, Lechel U, Veit R, Truckenbrodt R, Stamm G, Coppenrath EM. Assessment of a theoretical formalism for dose estimation in CT: an anthropomorphic phantom study. Eur J Radiol 2004; 14: 1275-84.

23. Zankl M. Methods for assessing organ doses using computational models. Radiat Prot Dosimetry 1998; 80: 207-12

24. Snyder WS, Ford MR, Warner GG. Estimates of specific absorbed fractions for photon sources uniformly distributed in various organs of a heterogeneous phantom. Tennessee: Health Physics Division, Oak Ridge National Laboratory.

25. International Commission on Radiation Units and Measurements (ICRU). Patient dosimetry for x rays used in medical imaging. Reports produced by the German National Research Center for Environment and Health (GSF). ICRU Report No. 74. Journal of ICRU 2005; 5(2): 80-86.

26. International Commission on Radiation Units and Measurements (ICRU). Patient dosimetry for x rays used in medical imaging. Reports produced by the National Radiological Protection Board (NRPB). ICRU Report No. 74. Journal of ICRU 2005; 5(2): 87-92.

27. Shrimpton PC, Jones DG. Normalised organ doses for x ray computed tomography calculated using Monte Carlo techniques and a mathematical anthropo-morphic phantom. National Radiological Protection Board. Radiat Prot Dosimetry 1993; 49: 241-3.

28. Hidajat N, Maurer J, Schroder RJ, Nunnemann A, Wolf M, Pauli K, et al. Relationship between physical dose quantities and patient dose in CT. Br J Radiol 1999; 72: 556-61.

29. Cohnen M, Poll LW, Puettmann C, Ewen K, Saleh A, Modder U. Effective doses in standard protocols for multi-slice CT scanning. Eur Radiol 2003; 13: 1148-53.

30. Van Der Molen AJ, Veldkamp WJH, Geleijns J. 16-slice CT: achievable effective doses of common protocols in comparison with recent CT dose surveys. Br J Radiol 2007; 80: 248-55.

31. Le Heron JC. CTDOSE. New Zealand: Ministry of Health, National Radiation Laboratory; 1993.

32. Imaging Performance Assessment of CT (ImPACT) CT Patient Dosimetry Calculator, version 0.99m. Created by 07/01/2002. Avaliable at: http:// www. impactscan .org/ctdosimitry.htm.

33. Stamm G, Nagel HD. CT-Expoein neuartiges Programm zur Dosisevaluierung In der CT. Fortschr Rontgenstr 2002; 74: 1570-76.

34. WinDose [computer program]. version 2.1a. Erlangen, Germany: Kalender WA, Schmidt B, Zankl M, Schmidt M; 1999

35. Kalender WA, Schmidt B, Zankl M, Schmidt M. A PC program for estimating organ dose and effective dose values in computed tomography. Eur Radiol 1999; 9: 555-62.

36. International Commission on Radiological Protection (ICRP). Recommendations of the ICRP Publication 60. Oxford: Pergamon Press; 1991.

37. Peter F. Investigation of patient dose from CT examination using the VIP-Man model. Faculty of Rensselaer Polytechnic Institute, Nuclear Engineering and Science. New York; 2001.

38. American Association of Physicists in Medicine (AAPM). Specification and Acceptance Testing of Computed Tomography Scanners. AAPM Report No. 39. New York: AAPM; 1993.

39. National Council on Radiation Protection and Measurements (NCRP). Quality Assurance for Diagnostic Imaging. NCRP Report No. 99. Bethesda: MD; 1995.

40. Catphan® 500 and 600 Manual. The Phantom Laboratory, Inc. New York; 2006.

41. Wyman AC, Lawson TL, Goodman LR. Transverse anatomy of the human thorax, abdomen, and pelvis: An atlas of anatomical radiological computed tomographic and ultrasonic correlation. 1st ed. The United Stated; 1978.

42. United Kingdom Accreditation Service (UKAS). The expression of uncertainty and confidence in measurement. 2nd ed. UKAS Publication; 2007.

43. International Atomic Energy Agency (IAEA). Dosimetry in diagnostic radiology: A international code of practice. Technical reports series No. 457. Vienna: IAEA; 2007.

APPENDIX

APPENDIX A

Grouping and determination of correction factors for sensitivity

The TLDs were classified into 21 groups and the average TL signal of all TLDs was 249.11 nC. The correction factors for sensitivity of each group were ranged in 0.58-1.88 as shown in Table A.1-A.4.

Table A.1 Correction factors for sensitivity of 21 groups of TLDs (1^{st}-5^{th} group)

Dosimeter ID	**TL signals (nC) in each group**				
	1	**2**	**3**	**4**	**5**
A	130.69	147.52	158.20	162.59	179.41
B	132.87	152.55		169.76	183.30
C	133.89			170.53	184.42
D				171.77	186.45
E				173.50	187.10
F				173.83	188.24
G				174.31	189.50
H				179.35	189.99
I					190.80
J					191.05
K					192.10
L					193.78
Mean ± SD	**132.49 ± 1.64**	**150.04 ± 3.56**	**158.20 ± 0.00**	**171.95 ± 4.79**	**188.01 ± 4.11**
CF	**1.88**	**1.66**	**1.57**	**1.45**	**1.32**

Table A.2 The correction factors for sensitivity of 21 groups of TLDs (6^{th}-10^{th} group)

Dosimeter ID	TL signals (nC) in each group				
	6	**7**	**8**	**9**	**10**
A	194.18	207.21	214.02	224.36	233.29
B	195.04	207.76	214.55	225.11	233.43
C	196.22	208.06	215.44	227.16	235.05
D	200.09	208.12	215.52	227.46	235.16
E	202.11	209.17	216.67	228.12	236.97
F	202.46	209.60	217.35	229.23	237.43
G	203.37	209.82	217.64	229.74	238.38
H	204.08	210.01	218.44	230.48	238.92
I	204.33	210.99	219.64	230.71	239.22
J	204.65	211.23	220.68	231.10	240.24
K	204.73	211.36	220.81	231.36	242.38
L	206.84	213.47	221.79	232.97	242.68
Mean ± SD	**201.51 ± 4.03**	**209.73 ± 1.46**	**217.71 ± 2.37**	**228.98 ± 2.39**	**237.76 ± 2.88**
CF	**1.24**	**1.19**	**1.14**	**1.09**	**1.05**

Table A.3 The correction factors for sensitivity of 21 groups of TLDs (11^{th}-15^{th} group)

Dosimeter ID	TL signals (nC) in each group				
	11	**12**	**13**	**14**	**15**
A	243.54	249.75	259.24	268.07	276.10
B	243.61	250.92	260.09	268.32	277.53
C	244.03	251.32	260.67	268.52	277.63
D	244.27	251.38	260.87	272.03	278.53
E	245.51	251.55	261.62	272.23	279.04
F	246.40	252.17	261.81	272.36	279.54
G	247.01	252.77	262.47	272.44	279.60
H	247.09	254.37	262.86	272.65	280.71
I	247.82	255.15	263.74	272.95	282.02
J	247.96	255.46	265.13	273.32	282.41
K	248.09	256.71	265.26	275.20	283.13
L	249.05	257.90	266.15	275.98	283.84
Mean ± SD	**246.20 ± 1.94**	**253.29 ± 2.57**	**262.50 ± 2.20**	**272.01 ± 2.53**	**280.01 ± 2.44**
CF	**1.01**	**0.98**	**0.95**	**0.92**	**0.89**

Table A.4 The correction factors for sensitivity of 21 groups of TLDs (16^{th}-21^{st} group)

Dosimeter ID	TL signals (nC) in each group					
	16	**17**	**18**	**19**	**20**	**21**
A	284.27	301.94	327.68	360.77	401.44	429.43
B	286.84	302.07	328.98	361.14		
C	287.59	307.88	331.44	362.17		
D	288.59	309.02	336.59	364.78		
E	292.88	311.14	337.00	368.82		
F	294.09	312.80	342.63	382.24		
G	295.03	313.13	345.60			
H	295.70	314.23	345.99			
I	296.17	314.46				
J	297.12	315.45				
K	297.49	317.61				
L	301.42	320.37				
Mean ± SD	**293.1 ± 5.16**	**311.68 ± 5.65**	**336.99 ± 7.26**	**366.65 ± 8.20**	**401.44 ± 0.00**	**429.43 ± 0.00**
CF	**0.85**	**0.80**	**0.74**	**0.68**	**0.62**	**0.58**

APPENDIX B

Absorbed doses and corresponding TLD signals in the TLD calibration

The absorbed doses and the corresponding TL signals derived from the TLD calibration are shown in Table B.

Table B Absorbed doses of 0.085-58.934 mGy and the corresponding TL signals

TL signal (nC)	Absorbed dose (mGy)
0.355	0.085
19.319	0.332
34.656	0.532
57.602	1.088
111.959	2.051
243.070	4.100
421.532	7.094
564.309	9.905
786.988	12.688
1424.160	22.446
2223.000	35.414
2783.154	47.288
3723.514	58.934

APPENDIX C

Determination of effective energy

The relationships between the CT numbers and the linear attenuation coefficients (μ) of Teflon, acrylic, and polystryrene are represented in Equation C.1-C.3

$$958.79 = \frac{1000(\mu_t - \mu_w)}{\mu_w} \quad \text{Equation C.1}$$

$$120.62 = \frac{1000(\mu_a - \mu_w)}{\mu_w} \quad \text{Equation C.2}$$

$$-37.69 = \frac{1000(\mu_p - \mu_w)}{\mu_w} \quad \text{Equation C.3}$$

To find the relationship equation among the linear attenuation coefficients of the three targets, the Equation C.2 was divided by the Equation C.1 and the Equation C.2 was divided by the Equation C.3. Then, Equation C.4 and C.5 were derived.

$$\frac{120.62}{958.79} = \frac{\mu_a - \mu_w}{\mu_t - \mu_w} \quad \text{Equation C.4}$$

$$\frac{120.62}{-37.69} = \frac{\mu_a - \mu_w}{\mu_p - \mu_w} \quad \text{Equation C.5}$$

The Equation C.4 was solved according to these following steps.

$$120.62(\mu_t - \mu_w) = 958.79(\mu_a - \mu_w)$$

$$120.62\,\mu_t - 120.62\,\mu_w = 958.79\,\mu_a - 958.79\,\mu_w$$

$$838.17\,\mu_w = 958.79\,\mu_a - 120.62\,\mu_t \quad \text{Equation C.6}$$

The Equation C.5 was solved according to these following steps.

$$120.62(\mu_p - \mu_w) = -37.69(\mu_a - \mu_w)$$

$$120.62\,\mu_p - 120.62\,\mu_w = -37.69\,\mu_a + 37.69\,\mu_w$$

$$158.31\,\mu_w = 120.62\,\mu_p + 37.69\,\mu_a \qquad \text{Equation C.7}$$

The Equation C.6 was divided by the Equation C.7

$$5.29 = \frac{958.79\,\mu_a - 120.62\,\mu_t}{120.62\,\mu_p + 37.69\,\mu_a}$$

$$638.08\,\mu_p + 199.38\,\mu_a = 958.79\,\mu_a - 120.62\,\mu_t$$

$$120.62\,\mu_t = 759.41\,\mu_a - 638.08\,\mu_p$$

Therefore, the relationship equation among the linear attenuation coefficients of the three targets shown in Equation C.8 was derived.

$$\mu_t = 6.29\,\mu_a - 5.29\,\mu_p \qquad \text{Equation C.8}$$

APPENDIX D

Determination of uncertainty of absorbed dose measurement by using TLD and dose calculation by using WinDose® program

The uncertainty of the absorbed dose measurement by using TLD and the dose calculation by using the WinDose® program were determined according to the United Kingdom Accreditation Service (UKAS) 2007 (42) and Technical Report series No. 457 from IAEA 2007 (43)

D.1 Determination of uncertainty of the absorbed dose measurement by using TLD

From the Table 4.1.1, the uncertainty budgets were derived from the following components.

1) TLD grouping and determination of correction factors for sensitivity

Uncertainty of the TLD grouping was derived from the following values.

1.1) Repeatability of each TLD

Standard deviation (SD) of mean reading of each TLD for three times, written as $s(\bar{x})$, was calculated by the following equation.

$$s(\bar{x}) = \frac{1}{\sqrt{n}} s(x_i) \qquad \text{Equation D.1}$$

Where n is the number of measurements.

$s(x_i)$ is the standard deviation of each TL signal calculated by the following equation.

$$s(x_i) = \sqrt{\frac{1}{n-1}\sum_{i=1}^{n}(x_i - \bar{x})^2} \qquad \text{Equation D.2}$$

Maximum SD and maximum SD of the mean reading resulting from the TLD grouping were 10.1% and 5.8%, respectively.

1.2) Standard deviation (SD) in each group of TLDs

Each group of TL signal were grouped with 3% SD of mean reading in each

group. The uncertainty of the TLD grouping was calculated by the following equation.

$$u = \sqrt{(u_1^2 + u_2^2)} \qquad \text{Equation D.3}$$

$$u = \sqrt{(5.8^2 + 3^2)} = 6.7\,\%$$

Where u_1 is the maximum SD of the mean reading

u_2 is the SD in each group of TLDs

Therefore, the uncertainty of TLD grouping and determination of correction factors for sensitivity was 6.7%.

2) TLD calibration

Uncertainty of the TLD calibration was derived from the following values.

2.1) Repeatability of TLD

TLDs were calibrated for three times and SD of mean reading of each TL signal was calculated according to the Equation D.1. Maximum SD and SD of the mean reading resulting from the TLD calibration were 4.3% and 2.5%, respectively.

2.2) Repeatability of ionization chamber

The absorbed doses were measured by using ionization chamber for five times and SD of mean reading of absorbed doses were calculated according to the Equation D.1. Maximum SD and SD of the mean reading resulting from the absorbed dose measurement were 0.8% and 0.4%, respectively.

3) Calibration factor of ionization chamber

From a calibration certificate No. 032830, the uncertainty of calibration factor of the ionization chamber model TM 30009 of PTW-Nomex is ± 5% corresponding to the double SD (k=2).

4) Measuring accuracy

Uncertainty of measuring accuracy was derived from the repeatability of TLD measurement in Alderson Rando phantom for three times. SD of mean reading of TL signals was calculated according to the Equation D.1. Maximum SD and SD of the mean reading resulting from the absorbed dose measurement by using the TLD in

Alderson Rando phantom were 11.4% and 6.6%, respectively.

From these uncertainty budgets, the uncertainty of TLD grouping and TLD calibration represent type B standard uncertainty of the dose measurement by using TLD. Their probability distributions are rectangular distributions and their divisors are square root of three. The uncertainty of calibration factor of ionization chamber represents type B standard uncertainty with a normal probability distribution. The divisor is its coverage factor of two quoted in the calibration certificate. The uncertainty of measuring accuracy of TLD measurement in Alderson Rando phantom represents type A uncertainty with normal probability distribution and its divisor is 1.

The values of uncertainty budgets were divided by their divisors as shown in Table 5.1.1. The combined uncertainty was calculated according to the following equation.

$$\text{Combined uncertainty} = \sqrt{(3.9^2 + 1.4^2 + 0.2^2 + 2.5^2 + 6.6^2)} \qquad \text{Equation D.4}$$

$$\text{Combined uncertainty} = 8\%$$

The combined uncertainty was multiplied by the coverage factor (k) of 2 corresponding to confidence limit of 95%. Therefore, the expanded uncertainty of the absorbed dose measurement by using TLD was 16%.

D.2 Determination of uncertainty of the dose calculation by using WinDose® program

From the Table 4.1.2, the uncertainty budgets were derived from the following components.

1) CT air kerma index

Uncertainty of the measurement of CT air kerma index was derived from the following values.

1.1) Repeatability of the measurement of CT air kerma index

The values of CT air kerma index were measured by using ionization chamber for five times and SD of mean reading of absorbed doses were calculated according to the Equation D.1. Maximum SD and SD of the mean reading resulting from the measurement of CT air kerma index were 1.2% and 0.6%, respectively.

1.2) Calibration factor of ionization chamber

The uncertainty of calibration factor of the ionization chamber model TM 30009 of PTW-Nomex is ± 5% corresponding to the double SD (k=2).

2) Determination of effective energy

Uncertainty of determination of effective energy was obtained from the repeatability of CatPhan phantom measurement for three times. SD of mean reading was calculated according to the Equation D.1. Maximum SD and SD of the mean reading resulting from the determination of effective energy were 5.2% and 3%, respectively.

3) WinDose® program

Uncertainty of the WinDose® program as taken from Zankl M., 1998 (24) in terms of an accuracy of calculated organ doses based on Monte Carlo simulation published by the GSF Report was ±10%.

From these uncertainty budgets, the repeatability of the CT air kerma index measurement represents type A standard uncertainty of the dose calculation by using the WinDose® program. Its probability distribution is a normal distribution with divisor of 1. The uncertainty of calibration factor of ionization chamber represented type B standard uncertainty with a normal probability distribution. The divisor is its coverage factor of two quoted in the calibration certificate. The repeatability of CatPhan® phantom measurement to determine the effective energy represents type A uncertainty with a normal probability distribution and its divisor is 1. The uncertainty of the WinDose® program taken from Zankl M., 1998 (23) represents type B standard uncertainty with rectangular probability distribution and the divisor is square root of three

The values of uncertainty budgets were divided by their divisors as shown in Table 5.1.2. The combined uncertainty was calculated according to the following equation.

$$\text{Combined uncertainty} = \sqrt{(0.6^2 + 2.5^2 + 3.0^2 + 5.8^2)} \quad \text{Equation D.5}$$

$$\text{Combined uncertainty} = 7\%$$

The combined uncertainty was multiplied by the coverage factor (k) of 2 corresponding to confidence limit of 95%. Therefore, the expanded uncertainty the dose calculation by using WinDose® program was 14%.

BIOGRAPHY

NAME Miss Woranut Iampa

DATE OF BIRTH 30 May 1983

PLACE OF BIRTH Nakornpathom, Thailand

INSTITUTIONS ATTENDED Mahidol University, 2005:
Bachelor of Science (Radiological Technology)
Mahidol University, 2008:
Master of Science (Radiological Technology)

HOME ADDRESS 12/1 Raikhing, Sampran, Nakornpathom
Tel. 034-318157
E-mail: woranut_nuch@hotmail.com